

1 A multi-model comparison of meteorological drivers of surface ozone 2 over Europe

3
4 Noelia Otero^{1,3}, Jana Sillmann², Kathleen A. Mar¹, Henning W. Rust³, Sverre Solberg⁴,
5 Camilla Andersson⁵, Magnuz Engardt⁵, Robert Bergström⁵, Bertrand Bessagnet⁶,
6 Augustin Colette⁶, Florian Couvidat⁶, Cournelius Cuvelier⁷, Svetlana Tsyro⁸, Hilde
7 Fagerli⁸, Martijn Schaap^{9,3}, Astrid Manders⁹, Mihaela Mircea¹⁰, Gino Briganti¹⁰, Andrea
8 Cappelletti¹⁰, Mario Adani¹⁰, Massimo D'Isidoro¹⁰, María-Teresa Pay¹¹, Mark
9 Theobald¹², Marta G. Vivanco¹², Peter Wind^{8,13}, Narendra Ojha¹⁴, Valentin Raffort¹⁵
10 and Tim Butler^{1,3}

11
12 ¹Institute for Advanced Sustainability Studies e.V., Potsdam, Germany

13 ²CICERO Center for International Climate Research, Oslo, Norway

14 ³Freie Universität Berlin, Institut für Meteorologie, Berlin, Germany

15 ⁴Norwegian Institute for Air Research (NILU), Box 100, 2027 Kjeller, Norway

16 ⁵SMHI, Swedish Meteorological and Hydrological Institute, Norrköping, Sweden

17 ⁶INERIS, Institut National de l'Environnement Industriel et des Risques, Verneuil en
18 Halatte, France

19 ⁷European Commission, Joint Research Centre (JRC), Ispra, Italy

20 ⁸MET Norway, Norwegian Meteorological Institute, Oslo, Norway

21 ⁹TNO, Netherlands Institute for Applied Scientific Research, Utrecht, the Netherlands

22 ¹⁰ENE-National Agency for New Technologies, Energy and Sustainable Economic
23 Development, Bologna, Italy

24 ¹¹Barcelona Supercomputing Center, Centro Nacional de Supercomputación, Jordi
25 Girona, 29, 08034 Barcelona, Spain

26 ¹²CIEMAT, Atmospheric Pollution Unit, Avda. Complutense, 22, 28040 Madrid, Spain

27 ¹³Faculty of Science and Technology, University of Tromsø, Tromsø, Norway

28 ¹⁴Max-Planck-Institut für Chemie, Mainz, Germany

29 ¹⁵CEREA, Joint Laboratory Ecole des Ponts ParisTech – EDF R&D, Champs-Sur-
30 Marne, France

31
32
33
34
35 **Abstract.** The implementation of European emission abatement strategies has led to
36 significant reduction in the emissions of ozone precursors during the last decade.
37 Ground level ozone is also influenced by meteorological factors such as temperature,
38 which exhibit interannual variability, and are expected to change in the future. The
39 impacts of climate change on air quality are usually investigated through air quality
40 models that simulate interactions between emissions, meteorology and chemistry.
41 Within a multi-model assessment, this study aims to better understand how air quality
42 models represent the relationship between meteorological variables and surface ozone
43 concentrations over Europe. A multiple linear regression (MLR) approach is applied to
44 observed and modelled time series across ten European regions in springtime and
45 summertime for the period of 2000-2010 for both models and observations. Overall, the
46 air quality models are in better agreement with observations in summertime than in
47 springtime, and particularly in certain regions, such as France, Mid-Europe or East-
48 Europe, where local meteorological variables show a strong influence on surface ozone
49 concentrations. Larger discrepancies are found for the southern regions, such as the

50 Balkans, the Iberian Peninsula and the Mediterranean basin, especially in springtime.
51 We show that the air quality models do not properly reproduce the sensitivity of surface
52 ozone to some of the main meteorological drivers, such as maximum temperature,
53 relative humidity and surface solar radiation. Specifically, all air quality models show
54 more limitations to capture the strength of the ozone-relative humidity relationship
55 detected in the observed time series in most of the regions, in both seasons. Here, we
56 speculate that dry deposition schemes in the air quality models might play an essential
57 role to capture this relationship. We further quantify the relationship between ozone and
58 maximum temperature (m_{o_3-T} , climate penalty) in observations and air quality models.
59 In summertime, most of the air quality models are able to reproduce reasonably well the
60 observed climate penalty in certain regions such as France, Mid-Europe and North Italy.
61 However, larger discrepancies are found in springtime, where air quality models tend to
62 overestimate the magnitude of observed climate penalty.

73 1. Introduction

74
75 Tropospheric ozone is recognised as a threat to human health and ecosystem
76 productivity (Mills et al. 2007). It is produced by photochemical oxidation of carbon
77 monoxide and volatile organic compounds (VOCs) in the presence of nitrogen oxides
78 ($NO_x=NO+NO_2$) (Jacob and Winner, 2009). While it is an important pollutant on a
79 regional scale, due to the long-range transport effect it may also influence air quality on
80 a hemispheric scale (Hedegaard et al, 2013, Monks et al., 2015). Previous studies have
81 shown that the reduction of emissions of ozone precursors, lead to a decrease in
82 tropospheric ozone concentrations in Europe (Solberg et al. 2005, Jonson et al. 2006).
83 However, there is also a large year-to-year variability due to weather conditions
84 (Andersson et al. 2007).

85
86 Ozone variability is strongly related to meteorological conditions. Significant
87 correlations between ozone and temperature have been associated with the temperature-
88 dependent lifetime of peroxyacetyl nitrate (PAN), and also due to the temperature
89 dependence of biogenic emission of isoprene (Sillman and Samson, 1995). Substantial
90 increases in surface ozone have been associated with high temperatures and stable
91 anticyclonic, sunny conditions that promote ozone formation (Solberg et al. 2008).
92 Moreover, its strong relationship with temperature represents a major concern, since
93 under a changing climate the efforts on new air pollution mitigation strategies might be
94 insufficient. This effect, referred to as the climate penalty (Wu et al., 2008), is expected
95 to play an important role in future air quality (Hendriks et al. 2016). Similarly,
96 increasing solar radiation leads to high levels of ozone, though with a weak correlation
97 (Dawson et al. 2007) and it has been suggested that it could reflect in part the
98 association of clear sky with high temperatures (Ordóñez et al., 2005). Humidity
99 influences photochemistry through reactions between water vapor and atomic oxygen

100 (Vautard et al. 2012). High levels of humidity are normally related to enhanced cloud
101 cover and thus reduced photochemistry (Dueñas et al. 2002, Camalier et al. 2007).The
102 relationship between ozone and relative humidity can be also explained by dry
103 deposition through stomatal uptake: under low levels of humidity plants close their
104 stomata, which reduce the biogenic uptake (Hodnebrog et al. 2012, Kavassalis and
105 Murphy, 2017). High wind speed is usually correlated with low ozone concentrations
106 due to enhanced advection and deposition, although the processes involved are complex
107 and studies from different regions reported weak or insignificant correlations (Dawson
108 et al., 2007, Jacob and Winner, 2009).

109
110 Chemistry transport models (CTMs) are one of the most common tools to investigate
111 the impacts of climate change on air quality (Jacob and Winner, 2009, Colette et al.
112 2015). Due to assumptions, parametrizations and simplifications of processes, the
113 models themselves are subject to large uncertainties (Manders et al. 2012), which have
114 been reflected in some regional differences in the magnitude of surface ozone response
115 to projected climate change (Andersson and Engardt, 2010). Thus, model biases when
116 compared to observations still remain a concern, especially in terms of the response of
117 air quality under future climate (Fiore et al. 2009, Rasmussen et al. 2012). Comparisons
118 between model outputs and measurements of available observational dataset are
119 essential to evaluate the models ability to reproduce observations. Discrepancies in the
120 outputs of CTMs can be due chemical and physical processes, fluxes (emissions,
121 deposition and boundary fluxes) and meteorological processes (Vautard et al. 2012,
122 Bessagnet et al. 2016). In particular, quantification and isolation of the effects of
123 meteorology on ozone is a challenge, due to the complex interrelation between ozone,
124 meteorology, emissions and chemistry (Solberg et al. 2015). Thus, evaluating air quality
125 models with respect the meteorological inputs is important given that meteorology
126 drives numerous chemical processes (Vautard et al. 2012). A number of studies have
127 evaluated the performance of the meteorological models that drive CTMs by comparing
128 them with observations of weather parameters relevant for air quality (Smyth et al.,
129 2006, Vautard et al. 2012, Brunner et al. 2014, Makar et al. 2015, Bessagnet et al.
130 2016).

131
132 Capturing observed sensitivities of ozone to meteorological factors is required to assess
133 the confidence in the models and their ability to reproduce the observed relationships
134 between pollutants and meteorology and better understand potential impacts under
135 climate change. However, only a few studies have used model simulations to analyse
136 ozone sensitivities to meteorological parameters. Davis et al. (2011) evaluated the
137 performance of the Community Multiscale Air Quality (CMAQ) model to reproduce the
138 ozone sensitivities to meteorology across Eastern US. Their results showed that the
139 model underestimated the observed ozone sensitivities to temperature and relative
140 humidity. Recently, Fix et al. (2017) examined the capability of the NRCM-Chem
141 model to capture the meteorological sensitivities of high/extreme ozone. Overall, they
142 found substantial differences between the modelled and the observed sensitivities of
143 high levels of ozone to meteorological drivers that were not consistent between the three
144 regions of study. Due to the complex interactions and processes, estimating the ozone
145 sensitivities to key meteorological variables remains a challenge. Thus, we aim to
146 examine the capabilities of a set of CTMs to reproduce the observed ozone responses to
147 meteorological variables. To our knowledge, this is the first multi-model evaluation that
148 compares observed and modelled meteorological sensitivities of ozone over Europe
149 using a set of regional air quality models.

150

151 The EURODELTA-Trends (EDT) exercise has been designed to better understand the
152 evolution of air pollution and assess the efficiency of mitigation strategies for
153 improving air quality. The EDT exercise allows the evaluation of the skill of regional
154 air quality models and quantification of the role of the different key driving factors of
155 surface ozone, such as emissions changes, long-range transport and meteorological
156 variability (more details on the EDT exercise can be found in Colette et al. 2017a).
157 Earlier phases of EURODELTA and other relevant modelling exercises, such as
158 AQMEII (Air Quality Model Evaluation International Initiative, Rao et al. 2009)
159 covered a short period of time of one year, while only a few studies assessed long-term
160 air quality but limited to one model (Vautard et al., 2006, Jonson et al. 2006, Wilson et
161 al. 2012), or utilised climate data rather than reanalysed meteorology (e.g. Simpson et
162 al., 2014; Colette et al., 2015). The EDT exercise presents a multi-model hindcast of air
163 quality over 2 decades (1990-2010), and thus offers a good opportunity to evaluate the
164 role of driving meteorological factors on ozone variability.

165

166 The present study provides a novel and simple method to evaluate the performance of
167 air quality models in terms of meteorological sensitivities of ozone. Specifically, our
168 analysis focuses on the European ozone season (April to September) over the years
169 2000-2010. The choice of this period is mainly motivated by the availability of the
170 observational dataset from Schnell et al. (2014, 2015) (see section 2.1). Within the EDT
171 framework, a recent report has presented the main findings on the long-term evolution
172 of air quality (Colette et al. 2017b). Part of these results was obtained from the analysis
173 of the 1990s (1990-2000) and 2000s (2000-2010) separately. We focus on the second
174 decade (2000-2010), for which the interpolated dataset of observed maximum daily 8-
175 hourly mean ozone (MDA8 O₃) used in this study was available. Similarly to Otero et
176 al. (2016), we apply a multiple linear regression approach to examine the
177 meteorological influence on MDA8 O₃. Statistical models are developed separately for
178 observational datasets and air quality models, with the primary focus on examining both
179 observed and simulated relationships between MDA8 O₃ and meteorological drivers .

180

181 The present paper is structured as follows. Section 2 describes the observational data as
182 well as the air quality models studied here. The methodology and the design of the
183 statistical models are introduced in section 3. Section 4 discusses the results and the
184 summary and conclusions are discussed in section 5.

185

186 2. Data

187

188 2.1. Observations

189

190 This study uses gridded MDA8 O₃ concentrations created with an objective-mapping
191 algorithm developed by Schnell et al. (2014). They applied a new interpolation
192 technique over hourly observations of stations from the European Monitoring and
193 Evaluation Programme (EMEP) and the European Environment Agency's air quality
194 database (AirBase) to calculate surface ozone averaged over 1° by 1° grid cells (see
195 Schnell et al., 2014, 2015). Otero et al. (2016) used this dataset for examining the
196 influence of synoptic and local meteorological conditions over Europe. This
197 interpolated product offers a possibility to establish a direct comparison between
198 observations and CTMs. However, it must be acknowledged that for some areas with a
199 low number of stations (i.e. the southeastern or northeastern European regions) the

200 values interpolated into the 1°x1° degree grid cells may not be representative of such
201 large scales. Recently, Ordóñez et al. (2017) and Carro-Calvo et al. (2017) have used
202 this product to assess the impact of high-latitude and subtropical anticyclonic systems
203 on surface ozone and the synoptic drivers of summer ozone respectively. They reported
204 inhomogeneities during some years for specific grid-cells (e.g. in the Balkans and
205 Sweden), which were excluded from their analysis. However, we did not observe a clear
206 shift when analysing the spatial averages of the time series of the MDA8 O₃ for those
207 particular regions (e.g. Balkans and Scandinavia) (Figs. S1, S2), Therefore our analysis
208 includes the whole dataset.

209

210 This study investigates the influence of observed meteorological variables on MDA8
211 O₃, based on the ERA-Interim reanalysis product provided by the European Centre for
212 Medium-Range Weather Forecasts (ECMWF) at 1°x1° resolution (Dee et al. 2011).
213 Meteorological reanalyses products are essentially model simulations constrained by
214 observations and they have been widely validated against independent observations.
215 Daily mean values are calculated as the mean of the four available time steps at 00, 06,
216 12, and 18UTC for 10m wind speed components (u and v) and 2m relative humidity.
217 Maximum temperature is approximated by the daily maximum of those time steps,
218 while daily mean surface solar radiation is obtained from the 3-hourly values provided
219 for the forecast fields.

220

221 2.2. Chemistry Transport Models (CTMs)

222

223 A set of state-of-the-art air quality models participating in the EDT exercise is used
224 here: LOTOS-EUROS (Schaap et al., 2008, Manders et al. 2017), EMEP/MSC-W
225 (Simpson et al., 2012), CHIMERE (Mailer et al., 2017), MATCH (Robertson et al.,
226 1999) and MINNI (Mircea et al., 2016). The domain of the CTMs extends from 17°W
227 to 39.8°E and from 32°N to 70°N and it follows a regular latitude-longitude projection
228 of 0.25x0.4 respectively. The main features of the CTM setup are largely constrained by
229 the EDT experimental protocol (e.g. meteorology, boundary conditions, emissions,
230 resolution, see Colette et al. 2017a for further details). For instance, the boundary
231 conditions were defined from a climatology of observational data for most of the
232 experiments of the EDT exercise (including the data used here). However, the
233 representation of physical and chemical processes and the vertical distribution differ in
234 the CTMs, as well as the vertical distribution of model layers (including altitude of the
235 top layer and derivation of surface concentration at 3m height in the case of EMEP,
236 LOTOS-EUROS and MATCH). Moreover, there were no specific constrains imposed
237 on biogenic emissions (including soil NO emissions), which are represented by most of
238 the models using an online module (Colette et al. 2017a). Since we aim here to
239 compare the modelled relationship between meteorology and surface ozone, prescribing
240 common features in the CTMs is particularly an advantage to identify potential sources
241 of discrepancies.

242

243 The CTMs were forced by regional numerical weather model simulations using
244 boundary conditions from the ERA-Interim global reanalysis (Dee et al., 2011). Most of
245 the CTMs used the same meteorological input data, with a few exceptions. Three of
246 them (EMEP, CHIMERE and MINNI) used input meteorology from the Weather
247 Research and Forecast Model (WRF) (Skamarock et al. 2008). LOTOS-EUROS and
248 MATCH used the input meteorology produced by RACMO2 (van Meijgaard, 2012) and
249 HIRLAM (Dahlgren et al. 2016), respectively. Unlike the rest of the regional weather

250 models, RACMO2 used in the EDT exercise excluded nudging towards ERA-Interim,
251 which might have some impact in the meteorological fields generated by RACMO2. A
252 summary of the CTMs and the corresponding sources of meteorological input data with
253 some of the main characteristics are given in Table 1. As with the observations, CTMs
254 and their meteorological counterpart were interpolated to a common grid with $1^\circ \times 1^\circ$
255 horizontal resolution. The use of a coarser resolution could have an impact in some
256 regions with a complex orography where airflow is usually controlled by mesoscale
257 phenomena (e.g. see-breeze and mountain-valley winds) or in regions characterized by
258 high emission densities (Schaap et al., 2015, Gan et al. 2016). In such cases the use of a
259 finer grid could be beneficial to capture the variability of local processes.

260
261 A set of meteorological parameters was selected from the meteorological input data for
262 the regression analyses. Similarly to the procedure with ERA-Interim, daily means are
263 obtained from the available time steps every 3 hours in the case of WRF and RACMO2,
264 and every 6 hours for HIRLAM for the following variables: 10m wind speed
265 components, 2m relative humidity and surface solar radiation. Maximum temperature is
266 also approximated by the daily maximum of those time steps.

267 268 **3. Multiple linear regression model**

269
270 Summertime usually brings favourable conditions for high near-surface ozone
271 concentrations, such as air stagnation due to high-pressure systems, warmer
272 temperatures, higher UV radiation, and lower cloud cover (Dawson et al. 2007). This
273 study attempts to better understand how CTMs represent the meteorological sensitivities
274 of ozone. To this aim, we use a multiple linear regression approach that can provide
275 useful information of sensitivities in the distribution of ozone concentration as a whole
276 (Porter et al., 2015).

277
278 A total of five meteorological predictors (Table 2) are selected based on the existing
279 literature that has shown their strong influence on ozone pollution (e.g. Bloomfield et al.
280 1996, Barrero et al. 2005, Camalier et al. 2007, Dawson et al. 2007, Andersson and
281 Engardt, 2010, Rasmussen et al. 2012, Davis et al. 2011, Doherty et al., 2013, Otero et
282 al. 2016). Moreover, it has been shown that the occurrence of air pollution episodes
283 might increase when the pollution levels of the previous day are higher than normal
284 (Ziomas et al. 1995). Then, apart from the meteorological predictors, we add the effect
285 of the lag of ozone (MDA8 from the previous day) in order to examine the role of ozone
286 persistence. Additionally, we include harmonic functions that capture the effect of
287 seasonality as in Rust et al. al (2009) and Otero et al. (2016), which is referred as “day”
288 in the MLRs (see Table 2).

289
290 For this study, we divide the European domain into 10 regions: England (EN), Inflow
291 (IN), Iberian Peninsula (IP), France (FR), Mid-Europe (ME), Scandinavia (SC), North
292 Italy (NI), Mediterranean (MD), Balkans (BA) and Eastern Europe (EA). These regions
293 are based on those defined in the recent ETC/ACM Technical Paper (Colette et al.
294 2017b). For our study, we further subdivide the original Mediterranean region (MD)
295 into a region covering the Balkans (BA), due to the strong influence of the ozone
296 persistence on MDA8 O₃ over this particular region as noted previously in Otero et al.
297 (2016). Figure 1 shows the spatial coverage of each region and Table 3 lists their
298 coordinates. As shown in Otero et al. (2016), the relative importance of predictors in the
299 MLRs shows distinct seasonal patterns. Here, multiple linear regression models (MLR,

300 hereafter) are developed for each region for two seasons: springtime (April-May-June,
 301 AMJ) and summertime (July-August-September, JAS). These seasons differ from the
 302 meteorological definition, but cover the period when surface ozone typically reaches its
 303 highest concentrations (i.e. April-September). Additionally, we analysed the impact of
 304 the seasons' definition by performing sensitivity tests using the meteorological seasons
 305 (i.e. March-May-April, MAM and June-July-August, JJA). As shown in Figs. S3 and S4
 306 (see Supplement), we found a stronger impact of some relevant key driving factors of
 307 ozone (e.g. temperature and relative humidity) when using the seasons defined above
 308 (AMJ and JAS) than when using the meteorological seasons. Therefore, we consider
 309 that our choice of 3-month periods that cover the whole ozone season is particularly
 310 useful for examining the impact of individual meteorological parameters when ozone
 311 levels are highest. Since the domains covered by observations and CTMs do not
 312 coincide exactly, we applied an observational-mask to use the same number of grid-
 313 cells for CTMs and observations. Data used to estimate parameters of the MLR were
 314 spatially averaged over each region. Thus, we compare MLRs developed separately for
 315 CTMs and observations for each region and season. The observational dataset contains
 316 the gridded MDA8 O₃ and the meteorology input from ERA-Interim, while the dataset
 317 for the CTMs contains the MDA8 O₃ from each one of them along with the
 318 corresponding meteorological input (LOTOS and RACMO2, CHIMERE and WRF,
 319 MATCH and HIRLAM) (see Table 1).

320

321 A MLR is built to describe the relationship between MDA8 O₃ (predictand) and a set of
 322 covariates (or predictors) describing seasonality, ozone persistence and the influence of
 323 meteorological fields (Table 2). A data series y_t , $t = 1, \dots, N$ (e.g. observations or CTM
 324 simulations) for a given region and season is conceived as a Gaussian random variable
 325 Y_t with varying mean μ_t and homogeneous variance σ^2 . The mean μ_t is described as a
 326 linear function of the covariates, i.e.

327

$$328 \quad Y_t \sim \mathcal{N}(\mu_t, \sigma^2),$$

$$329 \quad \mu_t = \beta_0 + \beta_{sin} \sin\left(\frac{2\pi}{365.25} d_t\right) + \beta_{cos} \cos\left(\frac{2\pi}{365.25} d_t\right) + \beta_{lag} y_{t-1} + \sum_{k=1}^K \beta_k x_{t,k} \quad (1)$$

330

331 with t indexing daily values and d_t referring to the day in the year associated with the
 332 index t . β_0 is a constant offset, β_{sin} and β_{cos} are the first order coefficient of a Fourier
 333 series (e.g. Rust et al. 2009, 2013, Fischer et al. 2017), β_{lag} describes the persistence
 334 with respect to the previous day concentration y_{t-1} ; if t is the first day in the late
 335 summer season (JAS, July 1st), y_{t-1} is the concentration of June 30th. Further regression
 336 coefficients β_k describe the linear relation to potential meteorological drivers (see table
 337 2). For covariates standardized to unit variance, the regression coefficients (β) are
 338 standardised coefficients giving the change in the predictand with the covariate in units
 339 of covariate standard deviation.

340

341 Following the same strategy as used in Otero et al. (2016), the MLRs are developed
 342 through several common steps: 1) starting with the full set of potentially useful
 343 components in the predictor, a stepwise backward regression using the Akaike
 344 Information Criterion (AIC) as a selection criterion removes successively those
 345 components in the predictor, which contribute least to the model performance; and 2) a
 346 multi-collinearity index known as variance inflation factor (VIF, Maindonald and Braun
 347 2006) is used to detect multi-collinearity problems in the predictor (i.e. high correlations

348 between two or more components in the predictor). Components with a VIF above 10
349 are left out of the predictor (Kutner et al 2004).

350

351 The statistical performance of each MLR (built separately from observations and
352 CTMs) is assessed through the adjusted coefficient (R^2) and the root mean square error
353 (RMSE). The R^2 estimates the fraction of total variability described by the MLR and the
354 RMSE gives the average deviation between model and observation obtained in the
355 MLR. We also examine the relative importance of the individual components in the
356 predictor. According to the method proposed by Lindeman et al (1980), the relative
357 importance of each predictor is estimated by its contribution to the R^2 coefficient
358 (Grömping 2007). We assess the sensitivities of ozone to the predictors through the
359 standardised coefficients obtained from the regression. These coefficients indicate the
360 changes in the ozone response to the changes in the predictors, in terms of standard
361 deviation. Thus, for every standard deviation unit increase (decrease) of a specific
362 predictor, the predictand (MDA8 O₃) will increase (decrease) the amount indicated by
363 its coefficient in standard deviation units,. The use of standardised coefficients allows
364 us to establish a direct comparison in the influence of individual predictors. The effect
365 of seasonality introduced by the harmonic functions (namely, “day”, table 2) is kept in
366 the MLRs (Eq. 1) for its usefulness in improving the power of the regression analysis,
367 however further explanation about the effect of the predictors focuses on the rest of the
368 variables.

369

370 4. Results and discussion

371

372 4.1. CTM performance by region

373

374 We compare the seasonal cycle of observations and CTM results through the time series
375 of daily averaged values of MDA8 O₃ from observations and CTMs for the whole
376 period (i.e. April-September, 2000-2010) spatially averaged over each region.
377 Furthermore, correlation coefficients between both CTMs and observations at each
378 region and season are used to quantify the CTM performance.

379

380 4.1.1. Seasonal cycle of MDA8 O₃

381

382 We examine the ozone seasonal cycle represented by both the observational and
383 modelled dataset. Figure 2 depicts daily averages during 2000-2010 of MDA8 O₃ at
384 each region for the CTMs and observations. In general, all CTMs are biased high
385 compared with observations. CTM results are visually closer to observations in the
386 northwestern regions (i.e. IN, EN and FR), while the spread becomes larger over the
387 southern and southeastern regions (i.e. BA, NI, MD). The IN, EN and SC regions show
388 the highest observed concentrations in the starting months (AMJ), which is not
389 generally well captured by most of the CTMs, which show a more flat timeline (e.g.
390 LOTOS, MATCH, CHIMERE). For example, in the SC region, some of the CTMs
391 underestimate the ozone concentrations in AMJ (i.e. CHIMERE and MINNI). The rest
392 of the regions show the highest observed concentrations in JAS, which is generally
393 overestimated by the CTMs. Models show discrepancies in the ozone seasonal cycle
394 when compared to each other and when compared against observations. For example,
395 we observed substantial differences in the southern regions, such as IP, MD and BA,
396 where the models show a considerable spread. In those regions, the CTMs exhibit a
397 different behaviour when compared to each other. For instance, the EMEP model shows

398 ozone peak concentrations in April, while CHIMERE and MINNI show a peak in July.
399 Overall LOTOS shows a relatively constant positive bias in all regions, more evident in
400 the MD and NI regions.

401

402

403 4.1.2. Correlation coefficients between modelled and observed time series

404

405 The correlation coefficients between the observed and modelled values of MDA8 O₃ at
406 each region and in each season are shown in Fig. 3. Overall, MDA8 O₃ from the CTMs
407 is better correlated with observations in JAS than in AMJ in the regions ME, NI, EA
408 and EN. As expected from inspection of the average time series (Fig. 2), the lowest
409 correlations between models and observations are found in BA, especially in AMJ for
410 all models. In particular, EMEP is negatively correlated with observations over this
411 region. As mentioned above, the larger discrepancies between CTMs and observations
412 found over BA might be attributed to a low density of observation sites from which the
413 interpolated dataset is derived, resulting in a lower quality or higher uncertainties of
414 such products (Schnell et al. 2014). The highest correlations in AMJ are obtained at the
415 following regions: ME; FR; NI; and EN for most of the models, except for EMEP for
416 which the highest correlation with observations was found in IN and SC. In general, the
417 models that are most closely correlated with observations are MATCH, MINNI and
418 CHIMERE, while LOTOS shows the lowest correlations, which could be partially due
419 to the use of a different set-up of the RACMO2 model, without nudging towards ERA-
420 Interim (section 2.2). These correlations reflect the patterns represented by the seasonal
421 cycle described above.

422

423 4.2. MLR performance

424

425 Figures 4 and 5 depict the statistical performance of each MLR in terms of R² and
426 RMSE (respectively) at the different regions for both seasons, AMJ and JAS. The R²
427 values indicate that all MLRs models (based on both observations and CTMs) are able
428 to explain more than 60% of the MDA8 O₃ variance in all regions. Overall, the MLRs
429 show a stronger fit in JAS than in AMJ in most of the regions (Fig. 4). The MLRs
430 appear to perform better in regions such as NI, ME, FR or EA, while the poorest
431 statistical performance is found in IN and EN. The results obtained from the CTM-
432 based MLRs show a similar performance to the observation-based MLRs in most of the
433 regions. The lowest RMSE values for most of the MLR are found in SC ranging
434 between 1 and 3 ppb, while EN shows the largest RMSE values. The MLRs from
435 MATCH and CHIMERE show the lowest RMSE values (1-3ppb) suggesting the best
436 statistical fit from a predictive point of view.

437

438 Both R² and RMSE metrics indicate that the statistical performance of MLRs for
439 observations and CTMs show distinct variations between seasons and regions. Overall,
440 better performances are found in JAS and in some regions (i.e. ME, NI, or FR) where
441 MLRs are able to describe more than the 80% of the variance in CTMs and
442 observations. This could be attributed to the major role of meteorology in summer
443 influencing local photochemistry processes of ozone production, while in spring long
444 range transport plays a stronger role (Monks, 2000, Tarasova et al. 2007). As it includes
445 the bias, the RMSE reveals more differences among the MLRs when compared to each
446 other (e.g. larger errors for LOTOS when compared to MATCH or CHIMERE).
447 However, it is interesting that in general all MLRs show a similar tendency when

448 evaluating the statistical performance, which indicate that observations-based and
449 CTMs-based MLRs present a similar statistical performance for modelling MDA8 O₃.
450 The ability of the CTMs to reproduce the influence of meteorological drivers on MDA8
451 O₃ is discussed in more detail below.

452 **4.3. Effects of drivers on ozone concentrations**

453
454 The analysis of the influence of the predictors in the MLRs reveals distinctive regional
455 patterns in both observation-based and CTM-based MLRs. In agreement with Otero et
456 al. (2016), here we also find that the regions geographically located towards the interior
457 (including central, western and eastern regions) appear to be more sensitive to the
458 meteorological predictors, especially in JAS. On the contrary, less meteorological
459 contribution is found in the regions over the northernmost and southernmost part of the
460 domain, implying that non-local processes (e.g. long-range transport) play a stronger
461 role here. Considering such similarities, in the following, the regions: EN, FR, ME, NI
462 and EA are referred as the internal regions, while the rest of the regions: IN, SC, IP, MD
463 and BA, are referred as the external regions (see Fig. 1).

464 4.3.1 Relative importance

465
466 Figure 6 depicts the relative importance of the predictors for the observation-based and
467 CTM-based MLRs in the internal regions (Fig. 1). Here, a larger meteorological
468 influence (i.e., the predictors other than LO3 and day) can be seen in JAS compared to
469 AMJ in all of these regions. In general, the dominant meteorological drivers from the
470 observation-based MLRs in these internal regions are RH and Tx. The contribution of
471 RH is evident in AMJ (e.g. ME, or EA), while Tx is clearly dominant in JAS. SSRD is
472 also a key driver of MDA8 O₃ and generally, the wind factors (W10m and Wdir) appear
473 to have a minor contribution.

474
475
476 Despite the CTM-based MLRs being able to capture the meteorological predictors, we
477 observe discrepancies among the internal regions when compared to the observation-
478 based MLR. The inter-model differences in terms of the relative importance of
479 predictors are greater in AMJ than in JAS. For instance, the contribution of the LO3 is
480 overestimated by most of CTMs. Substantial differences are found in the influence of
481 RH when comparing the observation-based and the CTMs-based models. The CTMs do
482 not capture the relative importance of the RH well, especially in AMJ. In general, the
483 CTMs driven by WRF meteorology show a slightly larger contribution of RH in most of
484 the cases, although we notice that there are also some differences among the models that
485 share the same meteorology. CTMs do capture the relative importance of Tx in all
486 regions, but overall they overestimate it, as they also show for SSRD. Here, we find
487 discrepancies when comparing the contribution of predictors in the statistical models
488 from CTMs driven by the same meteorology (e.g. EMEP when compared to CHIMERE
489 and MINNI). Such differences among the models using the same meteorology point out
490 that the model setup (e.g. number of vertical levels, depth of first layer) and model
491 parameterizations (e.g. chemistry/physical processes) have a larger influence in the
492 model performance than the meteorological processes.

493
494
495 Figure 7 presents the relative importance of individual predictors in the MLRs
496 developed at the external regions (Fig. 1) for both seasons. The observation-based
497 MLRs show that the main driving factor is LO3 in AMJ, while the effect of

498 meteorological drivers becomes stronger in JAS. RH presents a larger contribution in
499 some regions (e.g. IN, IP or SC) in AMJ and Tx in JAS (e.g. IN, IP, SC and BA). The
500 contribution of wind components, Wdir and W10m, is mainly reflected in both seasons
501 in the western regions (i.e. IN and IP) and in MD, respectively.

502
503 Overall, all CTMs show this tendency, although there are substantial differences when
504 comparing the individual drivers' contribution in the observation-based and CTM-based
505 MLRs, particularly in AMJ (Fig. 7). CTMs do not capture the contribution of LO3
506 reflected by the observation-based MLRs. As in the previous analysis (section 4.1) the
507 largest discrepancies are found in BA. In this region, the observation-based MLR shows
508 that most of the variability of ozone would be explained by LO3, while the CTM-based
509 MLRs underestimate the contribution of LO3 and overestimate the meteorological
510 contribution of Tx, SSRD and RH (e.g. LOTOS, CHIMERE and MINNI). The
511 contribution of RH is, again, underestimated by the CTMs in most of the regions,
512 (except in BA). On the contrary, the relative importance of SSRD is overestimated in
513 some regions (e.g. IP, IN or MD) and Tx (IN, SC), in particular for the CTMs driven by
514 WRF. Overall, CTMs show the observed contribution of W10m and Wdir in both
515 seasons, although with some inconsistencies among the regions and CTMs.

516
517 Our results indicate that the relative importance of meteorological factors is stronger in
518 the internal regions (Fig.6) than in the external regions (Fig.7), which could be partially
519 attributed to a larger variability of most of the meteorological fields in internal regions
520 (Fig. S5). The external regions are also more likely to be influenced by the lateral
521 boundary conditions applied by each CTM. In addition, in some external regions (e.g.
522 IP or MD), as mentioned in section 2, the use of a coarser grid in some regions might be
523 insufficient to capture mesoscale processes, such as land-sea breezes, which also control
524 MDA8 O₃ concentrations (Millán et al. 2002). Moreover, we observe that meteorology
525 becomes more important in summer, when local photochemistry processes are
526 dominant. In general, CTMs show this tendency, but limitations to reproduce the effect
527 of some meteorological drivers are found. Specifically, while CTMs tend to
528 overestimate the contribution of Tx, and SSRD, they underestimate the relative
529 importance of RH, which is also reflected in the correlations coefficients between
530 predictand the predictors (Figs. S6, S7).

531

532 4.3.2 Sensitivity of ozone to the drivers

533

534 We assess the sensitivities of MDA8 O₃ to the drivers through their standardised
535 coefficients obtained in the MLR (Section 3). These coefficients provide further
536 information about the changes of MDA8 O₃ due to the effect of each driver. Figures 8
537 and 9 depict the values of the main driving factors obtained in the MLR for the internal
538 and the external regions (respectively): LO3, Tx and RH. Similarly to those patterns
539 described by the relative importance of drivers, we observe that the ozone response to
540 LO3 is stronger in AMJ than in JAS: the corresponding standardised coefficients are
541 always positive and generally higher in AMJ. The observed sensitivities to LO3 are
542 smaller in the internal regions (Fig. 8), being particularly dominant in the external
543 regions (Fig. 9). Overall, most of the CTMs reflect a similar tendency. However, there
544 are evident differences between observations and CTMs when comparing the values of
545 the standardised coefficients, specifically in some regions such as BA or MD. When
546 comparing the ozone responses of the CTMs to LO3, we observe that in most of the

547 regions MATCH and MINNI show values closest to observations, which is consistent
548 with the results described at the beginning of this section (4.1.2).

549

550 Correlations between MDA8 O₃ and Tx are strong, especially in the internal regions in
551 JAS (Fig. S6). Overall, we show that the CTMs appear to capture the observed effect of
552 Tx better in JAS than in AMJ in most of the regions. The highest sensitivities to Tx are
553 found in internal regions such as ME, NI, FR and EN, which is also shown in the CTMs
554 (Fig. 8). However, we see that most of the CTMs tend to overestimate the effect of Tx
555 and distinct sensitivities to Tx are also found for those models that share the same
556 meteorology (i.e. CHIMERE, EMEP and MINNI). In particular, the MINNI and
557 CHIMERE models show higher Tx sensitivities when compared to the rest of the
558 CTMs. While the MINNI model presents the highest sensitivities to Tx in spring,
559 especially in EN and FR, EMEP shows smaller values and it underestimates the
560 correlations between Tx and MDA8 O₃ (Figs. S6, S7).

561

562 The slope of the ozone-temperature relationship (m_{O_3-T}) has been used in several studies
563 to assess the ozone climate penalty (eg. Bloomer et al., 2009, Steiner et al., 2010,
564 Rasmussen et al., 2012, Brown-Steiner et al. 2015) in the context of future air quality.
565 Thus, we additionally analyse the ozone-temperature relationship in order to provide
566 insight into the ability of CTMs to reproduce the observed m_{O_3-T} . Similarly to previous
567 work (Brown-Steiner et al. 2015), the slopes are obtained from a simple linear
568 regression using only Tx (without the influence from other predictors) and they are used
569 to quantify such relationship in both seasons, AMJ and JAS.

570

571 Figures 10 and 11 illustrate the m_{O_3-T} for the internal and the external regions
572 respectively. The observed m_{O_3-T} is larger in JAS than in AMJ. In AMJ, it ranges
573 between -0.45 and 1.15 ppbK⁻¹ with the largest values found in ME, NI and MD. In
574 JAS, the observed climate penalty is of the order of 1-2.7 ppbK⁻¹ with the largest values
575 in EN, FR, ME, NI, and MD. CTMs show a better agreement with observations in JAS
576 than in AMJ. CTMs tend to overestimate the climate penalty in AMJ in most of the
577 regions, with some exceptions, such as EMEP and MATCH that systematically
578 underestimate the slopes. Also, CTMs are generally better in simulating the observed
579 m_{O_3-T} in the internal regions compared to the m_{O_3-T} in the external regions, where in
580 general CTMs appear to overestimate the climate penalty in both seasons. Using this
581 metric, we identify some regions particularly sensitive to temperature, with larger
582 values of m_{O_3-T} (e.g. EN, ME, FR, NI or MD). Through a multi-model assessment,
583 Colette et al. (2015) showed a significant summertime climate penalty in southern,
584 western and central European regions (e.g. EA, IP, FR, ME or MD) in the majority of
585 the future climate scenarios used. Our study shows that most of the CTMs confirm the
586 observed climate penalty in JAS in such regions in the near present, although we found
587 that most of the CTMs overestimate the climate penalty in AMJ, especially in the
588 external regions.

589

590 We see a stronger effect of RH in AMJ than in JAS in the observations with the greatest
591 impact in the internal regions (e.g. EA, ME, NI, FR and EN), which is not well
592 represented by the CTMs (Figs. 8 and 9). As mentioned, CTMs underestimate the
593 strength of the correlations between ozone and relative humidity (Figs. S6, S7). This
594 general lack of sensitivity to RH could also partially explain the tendency for all CTMs
595 to show a high bias in simulated ozone compared with observations (Fig. 2). Among
596 the possible reasons for this inconsistency, we hypothesize that it can be related to the

597 fact that ozone removal processes can be associated with higher relative humidity levels
598 during thunderstorm activity on hot moist days, which might not be well captured by
599 CTMs. As previous studies pointed out (e.g. Andersson and Engardt, 2010), the impacts
600 of ozone dry deposition suggest that it may also play a role in explaining the problems
601 that CTMs show to reproduce the observed ozone-relative humidity relationship. With a
602 simple modelling approach, Kavassalis and Murphy (2017) found that the relationship
603 between ozone and relative humidity was better captured by the inclusion of the vapour
604 pressure deficit-dependent dry deposition, pointing out the relevance of detailed dry
605 deposition schemes in the CTMs.

606
607 High SSRD levels favour photochemical ozone formation and it is usually positively
608 correlated to ozone. In this case, CTMs also present some limitations to capture this
609 effect and they overestimated the sensitivities of ozone to SSRD (Figs. S8, S9). For
610 example, the observations show a lower and surprisingly negative effect of SSRD.
611 Although the correlations between SSRD and ozone are positive (see Figs. S6, S7), the
612 presence of other predictors in the regression may reverse the sign of the estimated
613 coefficient. The CTMs show a stronger sensitivity of ozone to SSRD and they
614 overestimate its influence on surface ozone. Similarly, the sensitivities to Wdir and
615 W10m are also overestimated by the CTMs, especially in AMJ (Figs. S8, S9).

616
617 Our analysis suggests that CTMs present more limitations to reproduce the influence of
618 meteorological drivers to MDA8 O₃ concentrations in the external regions than in the
619 internal regions, particularly in AMJ. Moreover, we find the largest discrepancies in
620 BA, where models show the poorest seasonal performance and correlation coefficients
621 (Figs. 2 and 3, respectively), probably due a low quality of the observational dataset.

622
623 Furthermore, LO₃ is the main driver over most of the external regions and explains a
624 large proportion to the total variability of MDA8 O₃, while meteorological factors play
625 a smaller influence. Lemaire et al. (2016) found a very low performance (based on R²)
626 over the British Isles, Scandinavia and the Mediterranean using a different statistical
627 approach that only included two meteorological drivers. They attributed this low skill to
628 the large influence over those regions of long-range transport of air pollution (Lemaire
629 et al. 2016). Our results confirm the small influence of the meteorological drivers over
630 those regions and the strong influence of the ozone persistence. Moreover, in the case of
631 the external regions of northern Europe, it could also be explained due to the dominance
632 of transport processes such as the stratospheric-tropospheric exchange or long-range
633 transport from the European continent, rather than local meteorology, particularly in
634 AMJ (Monks, 2000, Tang et al. 2009, Andersson et al. 2009).

635
636 Previous work suggested that local sources of NO_x and biogenic VOC (ozone
637 precursors) are important factors of summertime ozone pollution in the Mediterranean
638 basin (Richards et al. 2013). Moreover, some studies suggested that the local vertical
639 recirculation and accumulation of pollutants play an important role in ozone pollution
640 episodes in this region: during the nighttime the air masses are held offshore by land-sea
641 breeze, creating reservoirs of pollutants that are brought back the following day (Millán
642 et al. 20002, Jiménez et al. 2006, Querol et al. 2017). All of these factors (e.g. local
643 emissions as well as local and large-scale processes) control the ozone variability,
644 which might explain the smaller influence of local meteorological factors shown in this
645 study over the Mediterranean basin when compared to meteorological influence in the
646 internal regions. Thus, we may hypothesize that the strong impact of LO₃ observed in

647 the external regions over southern Europe (i.e. IP, MD, BA) could be partially due to
648 the role of vertical accumulation and recirculation of air masses along the
649 Mediterranean coasts as a result of the mesoscale phenomena, which is enhanced by the
650 complex terrains that surround the Basin. Other important factor for the strong impact
651 of LO₃ observed is the slow dry deposition of ozone on water that would favour the
652 ozone persistence in southern Europe.

653

654 Overall we conclude that CTMs capture the effect of meteorological drivers better in the
655 internal regions (EN, FR, ME, NI and EA), where the influence of local meteorological
656 conditions is stronger. The major effect of meteorological parameters found in the
657 internal European regions might be also attributed to the fact that overall the variability
658 of meteorological conditions is larger in those regions (Fig. S5). We also find
659 differences among the CTMs driven by the same meteorology. As mentioned in the
660 introduction, Bessagnet et al. (2016) suggested that the spread in the model results
661 could be partly explained by the differences in the vertical turbulent mixing in the
662 planetary boundary layer, differently diagnosed in each of the CTMs. Our results also
663 indicate that even though models share the same meteorology (considering the
664 prescribed requirements defined by the EDT exercise) they show discrepancies when
665 compared to each other, which could be attributed to other sources of uncertainties
666 (such as physical and chemical internal processes in the CTMs). The NMVOC and NO_x
667 emissions from the biosphere are critical in the ozone formation. Since biogenic
668 emissions were not specifically prescribed, which have a strong dependence on
669 temperature and solar radiation, discrepancies in the CTMs performances, (e.g. different
670 sensitivities to Tx) might be expected. Furthermore, we notice that the CTMs do not
671 reproduce consistently the regional ozone-temperature relationship, which is a key
672 factor when assessing the impacts of climate change on future air quality.

673

674 **5. Summary and conclusions**

675

676 The present study evaluates the capabilities of a set of Chemical Transport Models
677 (CTMs) to capture the observed meteorological sensitivities of daily maximum 8-hour
678 average ozone (MDA8 O₃) over Europe. Our study reveals systematic differences
679 between the CTMs in reproducing the seasonal cycle when compared to observations.
680 In general, CTMs tend to overestimate the MDA8 O₃ in most of the regions. In the
681 western and northern regions (i.e. Inflow, England and Scandinavia), some models did
682 not capture the high ozone levels in spring (e.g. CHIMERE and MINNI), while in some
683 southern regions (e.g. Iberian Peninsula, Mediterranean and Balkans) they
684 overestimated the ozone levels in summer (e.g. LOTOS, CHIMERE). Of the CTMs,
685 MATCH and MINNI were the most successful in capturing the observed seasonal cycle
686 of ozone in most regions. All CTMs revealed limitations to reproduce the variability of
687 ozone over the Balkans region, with a general overestimation of the ozone
688 concentrations, considerably larger during the warmer months (July, August). As
689 reflected in the results, a limitation of the interpolated observational product used here
690 is that in some regions (e.g. southern Europe) it has a lower quality due to a reduced
691 number of stations (section 2.1).

692

693 The MLRs performed similarly for most of the CTMs and observations, describing
694 more than 60 % of the total variance of MDA8 O₃. Overall, the MLRs perform better in
695 JAS than in AMJ, and the highest percentages of described variance were found in Mid
696 Europe and North Italy. This could be attributed to local photochemical processes being

697 more important in JAS, and is consistent with a relatively stronger influence of long-
698 range transport in AMJ.

699

700 The effects of predictors revealed spatial and seasonal patterns, in terms of their relative
701 importance in the MLRs. Particularly, we noticed a larger local meteorological
702 influence in the regions located towards the interior of Europe, here termed as the
703 internal regions (i.e. England, France, Mid-Europe, North Italy and East-Europe). A
704 minor local meteorological contribution was found in the remaining regions, referred as
705 the external regions (i.e. Inflow, Iberian Peninsula, Scandinavia, Mediterranean and
706 Balkans). The CTMs are in better agreement with the observations in the internal
707 regions than in the external regions, where they were not as successful in reproducing
708 the effects of the ozone drivers. Overall, the different behaviour in the MLRs developed
709 in the external regions could be attributed to (i) a larger influence of dynamical
710 processes rather than local meteorological processes (e.g. long range transport in the
711 northern regions) (ii) a stronger impact of the boundary conditions (iii) the use of a
712 coarser grid that might be insufficient to capture mesoscale processes that also influence
713 MDA8 O₃ (e.g. sea-land breezes in the southern regions).

714

715 We found substantial differences in the sensitivities of MDA8 O₃ to the different
716 meteorological factors among the CTMs, even when they used the same meteorology.
717 As Bessagnet et al. (2016) point out, the differences amongst CTMs could be partly
718 attributed to some other diagnosed model variables (e.g. vertical turbulent mixing and
719 boundary layer height, as well as vertical model resolution). To assess the effect of such
720 potential sources of uncertainties, further investigations would be required. Moreover,
721 variations in the sensitivity of ozone to meteorological parameters could depend on
722 differences in the chemical and photolysis mechanisms and the implementation of
723 various physics schemes, all of which differ between the CTMs (see Colette et al.
724 2017a). Specifically, the discrepancies found in the sensitivities of MDA8 O₃ to
725 maximum temperature might be also attributed to biogenic emissions not prescribed in
726 the models. This was particularly reflected in the analysis of the slopes ozone-
727 temperature (m_{O_3-T}) to assess the climate penalty, which differed between CTMs and
728 regions when compared to the observations in both seasons. Most of the CTMs confirm
729 the observed climate penalty in JAS, but with larger discrepancies in the external
730 regions than in the internal regions. Furthermore, CTMs tend to overestimate the
731 climate penalty in AMJ (particularly in the external regions).

732

733 Our results have shown discrepancies in the observed and simulated ozone sensitivities
734 to relevant meteorological parameters for ozone formation and removal processes. In
735 particular, we found that CTMs tend to overestimate the influence of maximum
736 temperature and surface solar radiation in most of the regions, both strongly associated
737 with ozone production. None of the CTMs captured the strength of the observed
738 relationship between ozone and relative humidity appropriately, underestimating the
739 effect of relative humidity, a key factor in the ozone removal processes. We speculate
740 that ozone dry deposition schemes used by the CTMs in this study may not adequately
741 represent the relationship between humidity and stomatal conductance, thus
742 underestimating the ozone sink due to stomatal uptake. Further sensitivity analyses
743 would be recommended for testing the impact of the current dry deposition schemes in
744 the CTMs.

745

746 **Data availability**

747

748 The data are available upon request from the corresponding author.

749

750 **Acknowledgments**

751

752 We acknowledge Jordan L. Schnell for providing the interpolated dataset of MDA 8 O₃.
753 Modelling data used in the present analysis were produced in the framework of the
754 EURODELTA-Trends Project initiated by the Task Force on Measurement and
755 Modelling of the Convention on Long Range Transboundary Air Pollution.
756 EURODELTA-Trends is coordinated by INERIS and involves modelling teams of
757 BSC, CERE, CIEMAT, ENEA, IASS, JRC, MET Norway, TNO, SMHI. The views
758 expressed in this study are those of the authors and do not necessarily represent the
759 views of EURODELTA-Trends modelling teams. The MATCH participation was partly
760 funded by the Swedish Environmental Protection Agency through the research program
761 Swedish Clean Air and Climate (SCAC) and NordForsk through the research
762 programme Nordic WelfAir (grant no. 75007).

763

764

765

766

767

768

769

770

771

772

773

774

775

776

777

778

779

780

781

782

783

784

785

786

787

788 **List of Tables:**

Table 1. Summary of the chemistry-transport models used in the study and the main characteristics (adapted from Colette et al. 2017).

Model	Meteorological driver	Research group	Vertical layers (vl) Vertical extent (ve) Surface concentration (sc) Depth first layer (dl)	Biogenic VOC	Dry deposition (dd) Stomatal resistance (sr)	Land use database(lu) Advection scheme (ad) Vertical diffusion (vd)
CHIMERE	WRF (common driver)	INERIS	vl: 9 sigma ve: surface to 500 hPa sc: First model level dl: 20m	MEGAN model v2.1 with highresolution spatial and temporal leaf area index (LAI; Yuan et al., 2011) and recomputed emissions factors based on the land use (Guenther et al., 2006)	dd: Resistance model (Emberson et al., 2000a, b) sr: Emberson et al. (2000a, b)	lu: GLOBCOVER (24 classes) ad: van Leer (1984) vd: vertical diffusion coefficient (Kz) approach following Troen and Mahrt (1986)
EMEP	WRF (common driver)	MET Norway	vl: 20 sigma ve: surface to 100 hPa sc: Downscaled to 3 m dl: 90m	Online emissions based upon maps of 115 species from Koeble and Seufert (2001), and hourly temperature and light using Guenther et al. (1993, 1994). See Simpson et al. (1995, 2012)	dd: Resistance model for gases (Venkatram and Pleim, 1999); for aerosols: Simpson et al. (2012) sr: DO3SEEMEP: Emberson et al. (2000a, b), Tuovinen et al. (2004), Simpson et al. (2012)	lu: CCE/SEI for Europe, elsewhere GLC2000 ad: Bott (1989) vd: Kz approach following O'Brien (1970) and Jeriřceviř et al. (2010)
LOTOS-EUROS	RACMO2	TNO	vl: 5 (4 dynamic layers and a surface layer) ve: 5000 m sc: Downscaled to 3 m dl: 25m	Based upon maps of 115 species from Koeble and Seufert (2001), and hourly temperature and light (Guenther et al., 1991, 1993). See Beltman et al. (2013)	dd: Resistance model, DEPAC3.11 for gases, Van Zanten et al. (2010) and Zhang et al. (2001) for aerosols rs: Emberson et al. (2000a, b)	lu: Corine Land Cover 2000 (13 classes) ad: Walcek (2000) vd: Kz approach Yamartino et al. (2004)
MATCH	HIRLAM EURO4M	SMHI	vl: 39 hybrid levels of the meteorological model layers ve: surface to ca. 5000 m (4700–6000 m) sc: Downscaled to 3 m dl: ca. 60m	Online emissions based on Simpson et al. (2012), dependent on hourly temperature and light	dd: Resistance model depending on aerodynamic resistance and land use (vegetation). Similar to Andersson et al. (2007) sr: Simple, seasonally varying, diurnal variation of surface resistance for gases with stomatal resistance (similar to Andersson et al., 2007 and Simpson et al., 2012)	lu: CCE/SEI for Europe ad: Fourth-order massconserved advection scheme based on Bott (1989) vd: Implicit mass conservative Kz approach (see Robertson et al., 1999); Boundary layer parameterisation as detailed in Robertson et al. (1999) forms the basis for vertical diffusion and dry deposition
MINNI	WRF (common driver)	ENEA/Arianet S.r.l	vl: 16 fixed terrain-following layers ve: 10 000m sc: First model level dl: 40m	MEGAN v2.04 (Guenther et al., 2006)	dd: Resistance model based on Wesely (1989) sr: Wesely (1989)	lu: Corine Land Cover 2006 (22 classes) ad: Blackman cubic polynomials (Yamartino,1993) vd: Kz approach following Lange (1989)

791
792

Predictor	Definition	793
LO3	Lag of MDA8 O ₃ (24 h)	794
Tx	Maximum temperature	795
RH	Relative humidity	796
SSRD	Surface solar radiation	797
Wdir	Wind direction	798
W10m	Wind speed	799
day	$\sin(2\pi d_t/365.25)$,	800
	$\cos(2\pi d_t/365.25)$	801
		802

803
804
805
806

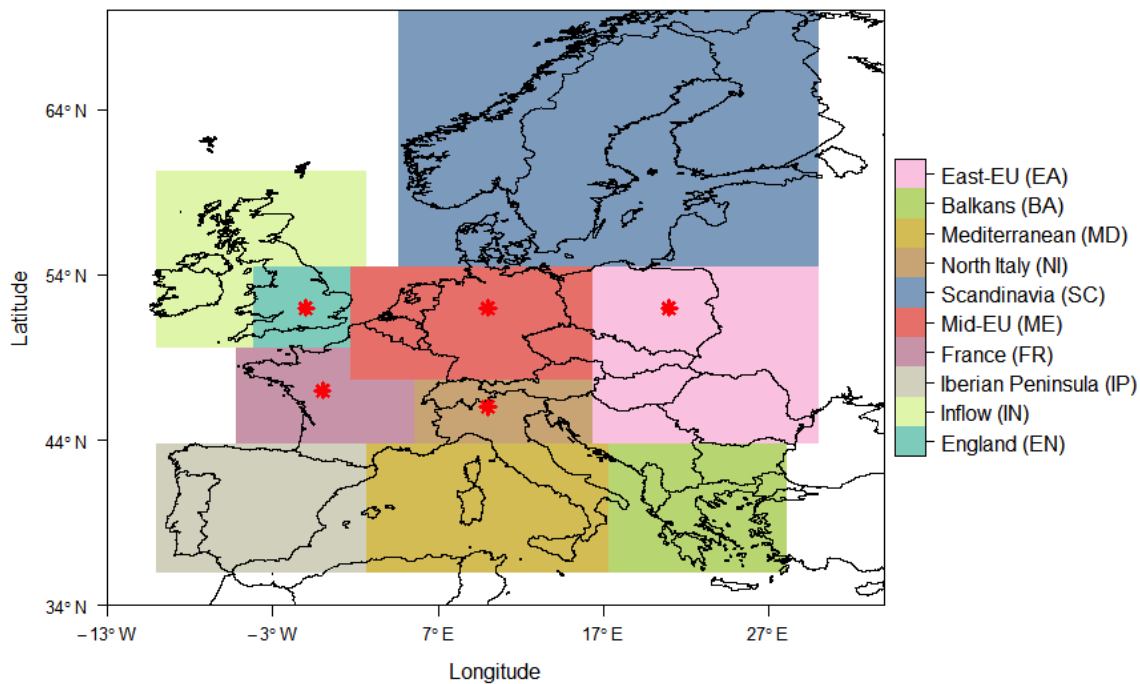
Table 2. List of the predictors used in the multiple linear regression analysis: meteorological parameters, lag of MDA8 O₃ (24h, previous day) and the seasonal cycle components.

Region	Acronym	Coordinates (longitude, latitude)	807
England	EN	5W-2E, 50N-55N	808
Inflow	IN	10W-5W, 50N-60N, and 5W-2E, 55N-60N	809
Iberian Peninsula	IP	10W-3E, 36N-44N	810
France	FR	5W-5E, 44N-50N	811
Mid-Europe	ME	2E-16E, 48N-55N	812
Scandinavia	SC	5E-16E, 55N-70N	813
North Italy	NI	5E-16E, 44N-48N	814
Balkans	BA	18E-28E, 38N-44N	815
Mediterranean	MD	3E-18E, 36N-44N	816
Eastern Europe	EA	16E-30E, 44N-55N	817
			818
			819
			820
			821

822
823
824
825
826
827
828
829
830
831
832
833
834
835
836
837
838
839
840
841
842
843

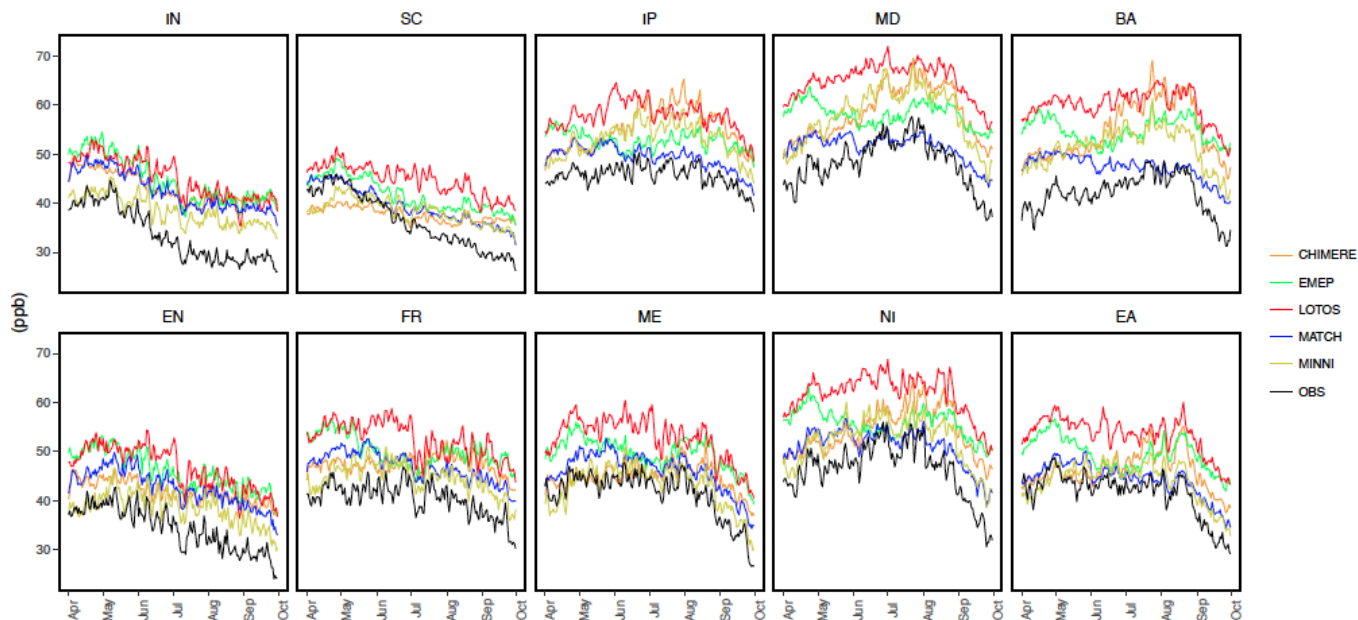
Table 3. List of the regions with the short name and the coordinates.

844 **List of Figures:**
 845



846
 847
 848
 849
 850
 851
 852

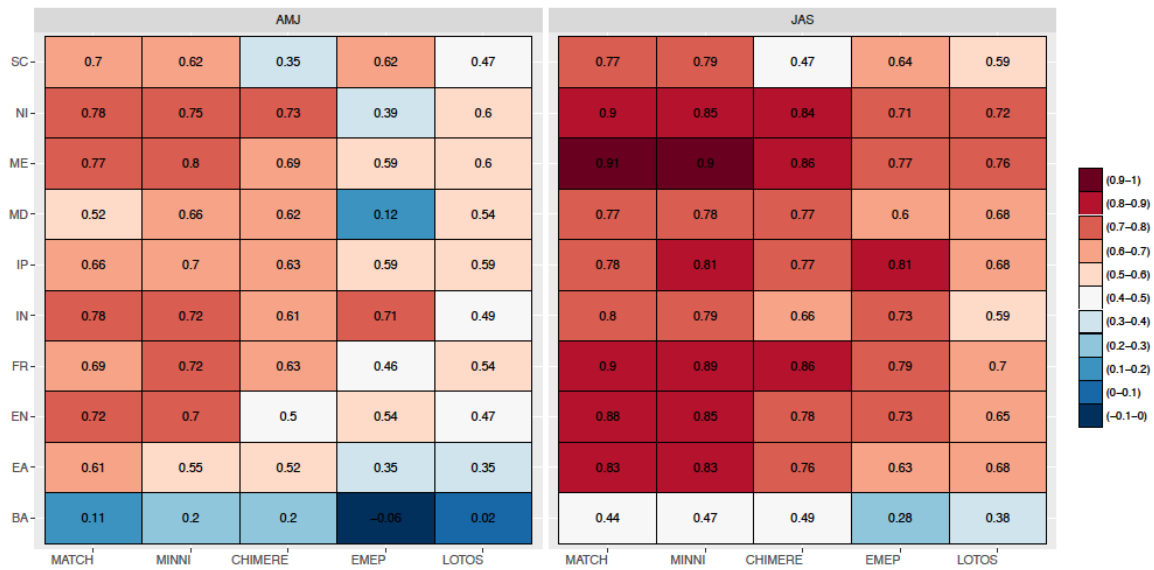
Figure 1. Map of the regions considered in the study. Regions indicated with a black star are referred to the internal regions in the text. The rest of regions are referred to the external regions of the European domain.



853
 854
 855
 856
 857

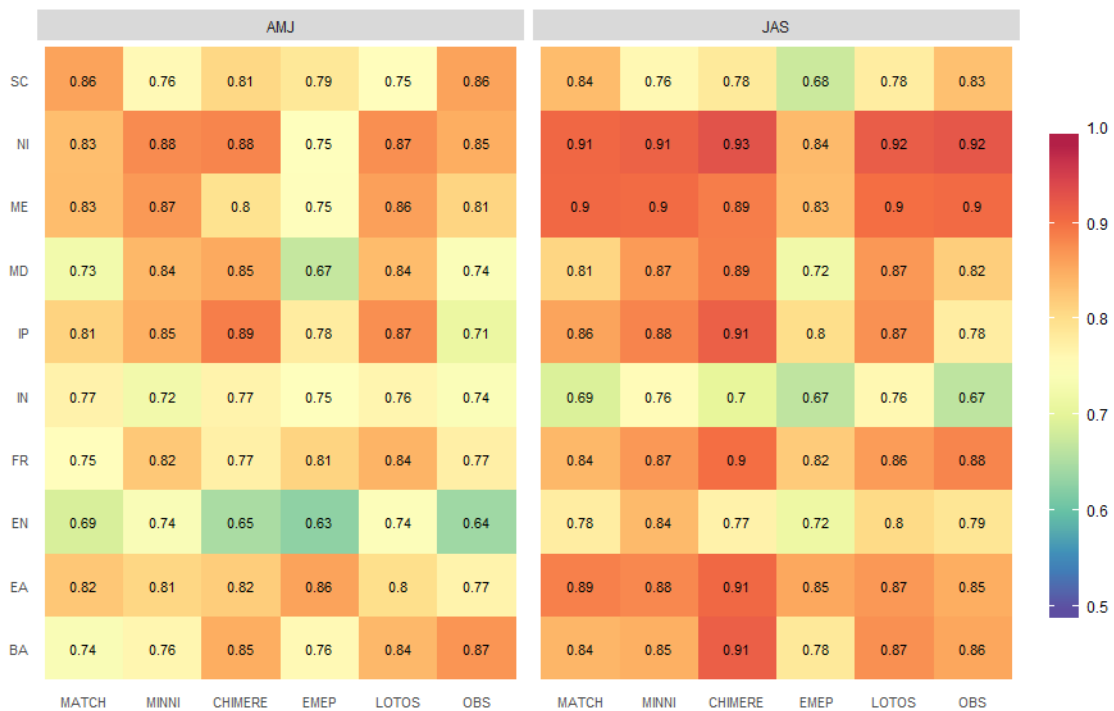
Figure 2. Time series of daily averages of MDA8 O₃ during the ozone season (April-September) for the period of study (2000-2010) at each subregion.

858
859



860
861
862
863
864
865
866

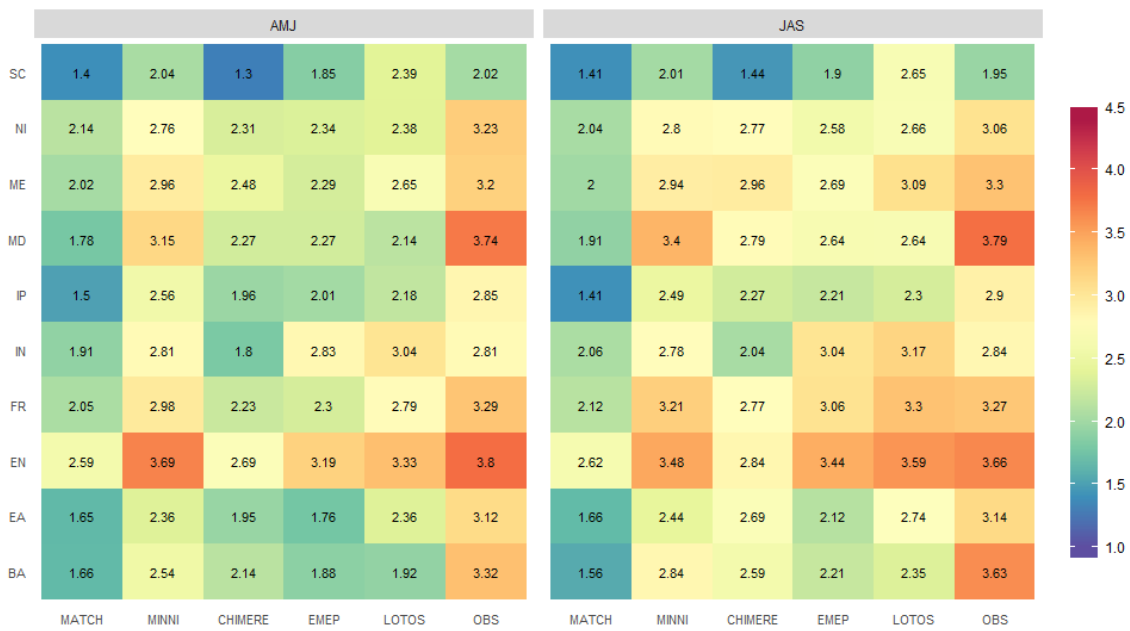
Figure 3. Correlation coefficients between observed and modelled MDA8 O₃ for spring (AMJ) and summer (JAS) for the period of study (2000-2010) at each region (rows) and model (columns, ordered by highest correlation values).



867
868
869
870
871
872
873
874
875
876
877

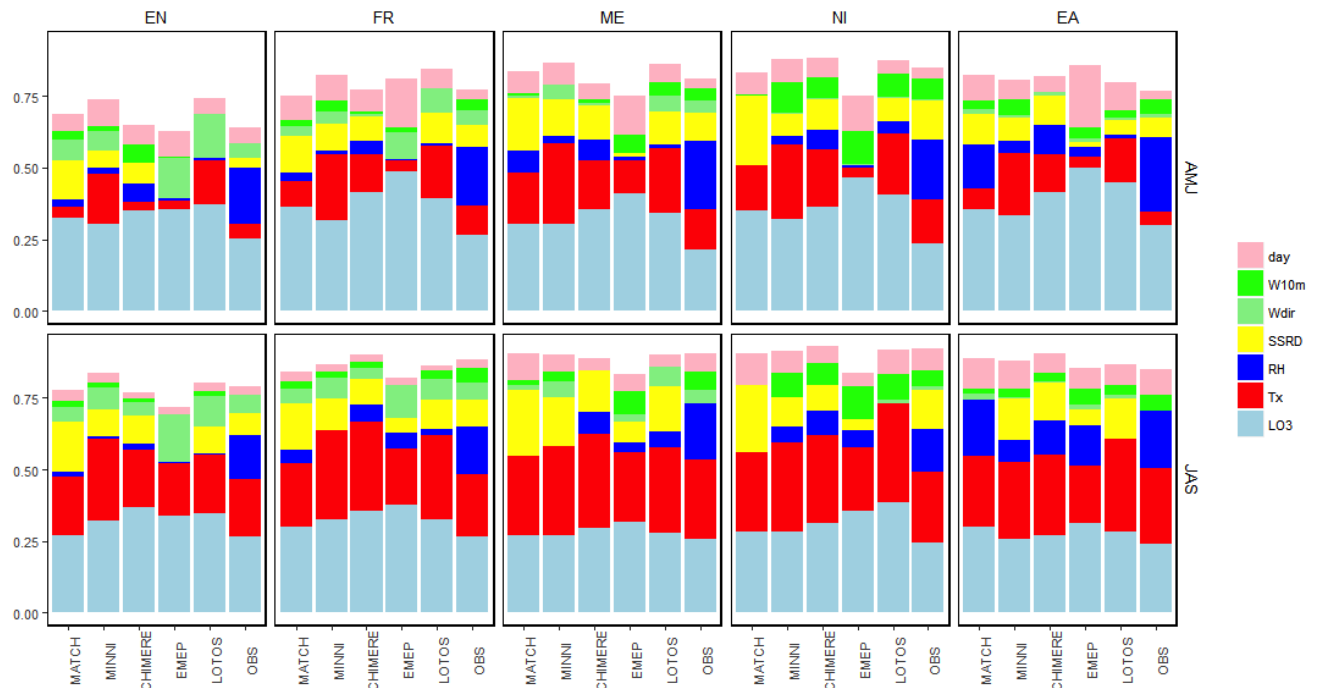
Figure 4. Coefficients of determination (R^2) for each CTM-based (ordered as in Fig.3) and observation-based MLR in spring (AMJ) and summer (JAS).

878
879



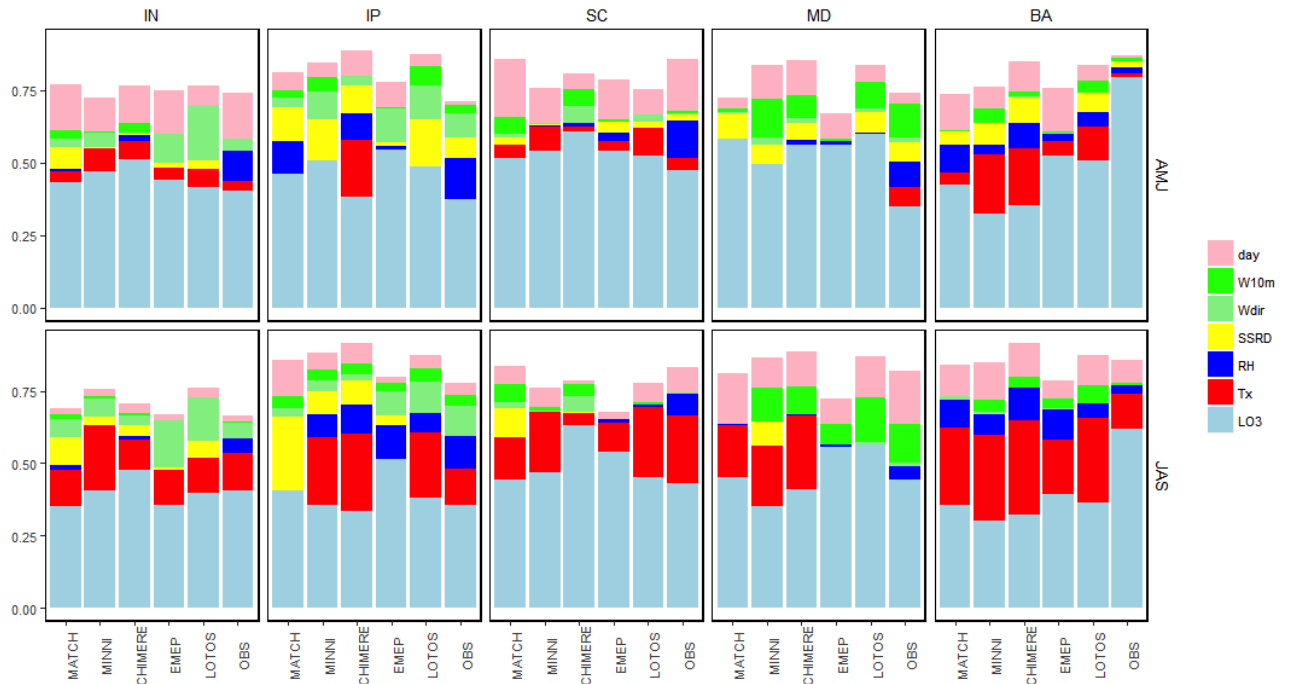
880
881
882
883
884
885
886

Figure 5. Root mean square errors (RMSE) for each CTM-based (ordered as in Fig.3) and observation-based MLR at each region, in spring (AMJ) and summer (JAS).



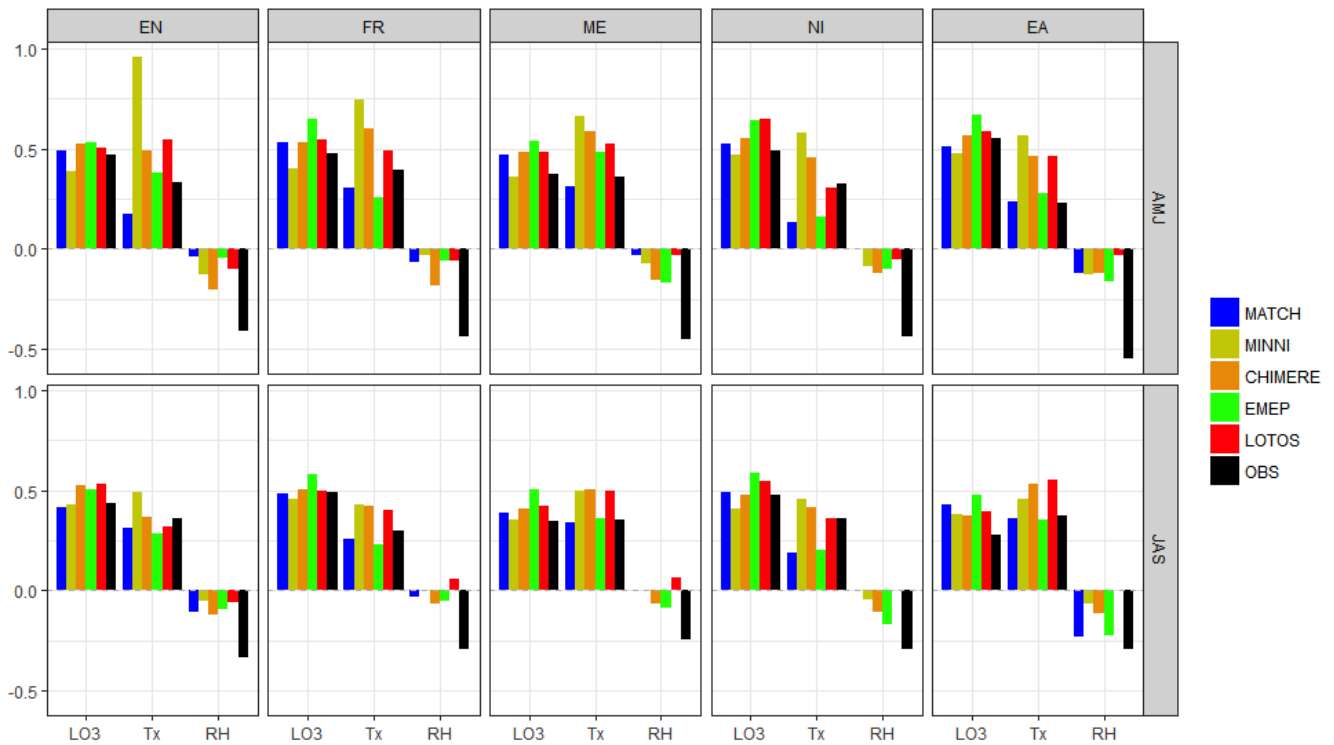
887
888
889
890
891
892

Figure 6. Proportion of each predictor to the total explained variance for each CTM-based (ordered as in Fig.3) and observation-based MLR in AMJ (top) and JAS (bottom) for the internal regions: England (EN), France (FR), Mid-Europe (ME), North Italy (NI) and East-Europe (EA).



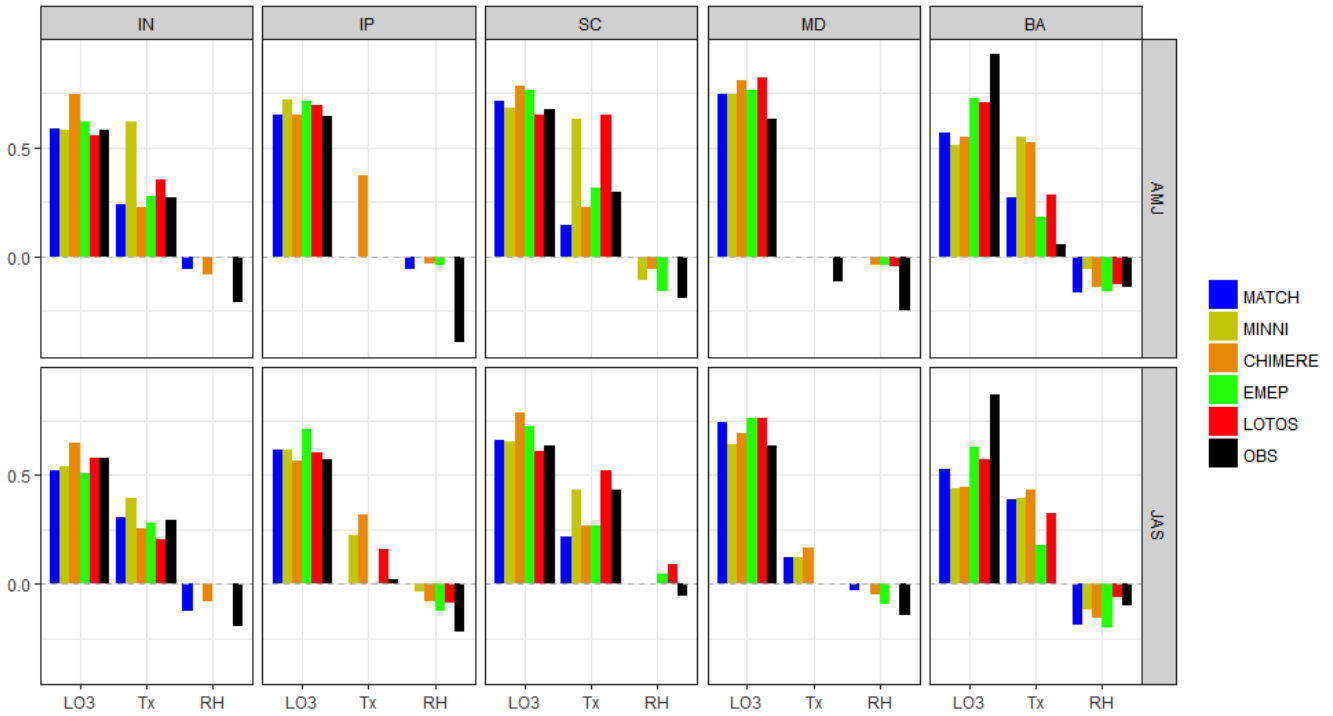
894
895
896
897
898
899
900

Figure 7. Proportion of each predictor to the total explained variance for each CTM-based (ordered as in Fig.3) and observation-based MLR in AMJ (top) and JAS (bottom) for the external regions: Inflow (IN), Iberian Peninsula (IP), Scandinavia (SC), Mediterranean (ME) and Balkans (BA).



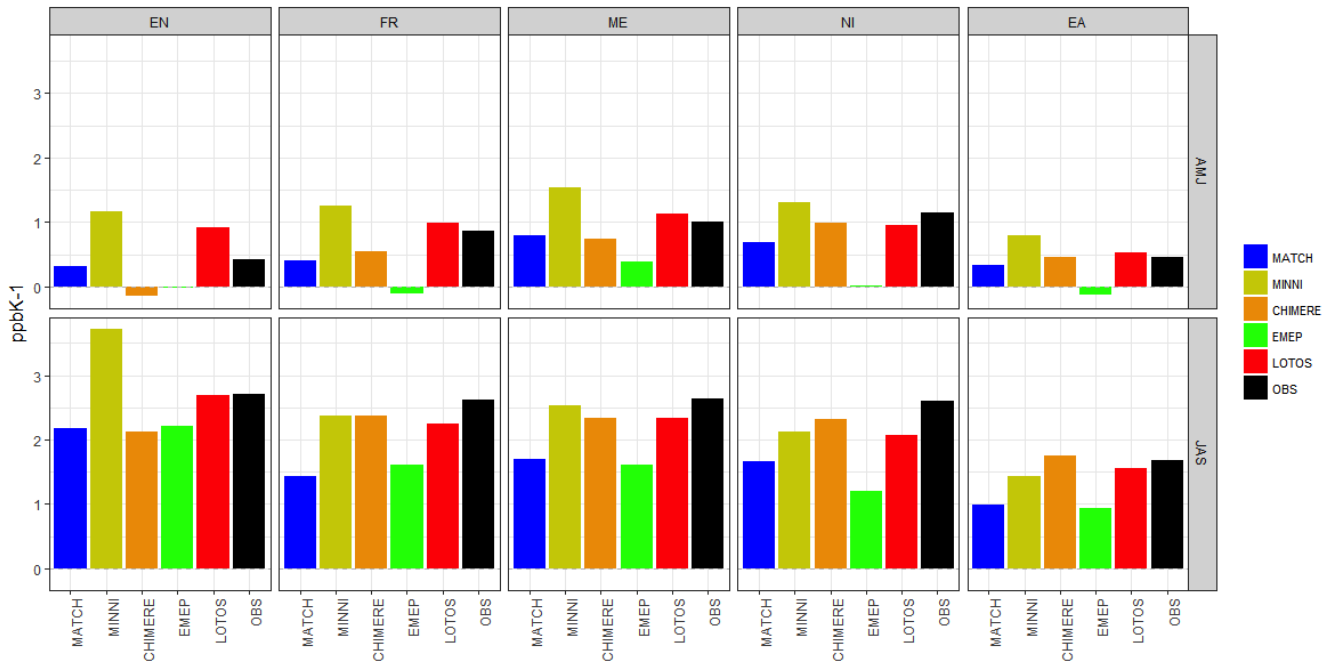
901
902
903
904
905
906

Figure 8. Standardised coefficients values of the main key-driving factors (LO3, Tx and RH) for each CTM-based (ordered as in Fig.3) and observation-based MLR in AMJ (top) and JAS (bottom) and for the internal regions: England (EN), France (FR), Mid-Europe (ME), North Italy (NI) and East-Europe (EA).



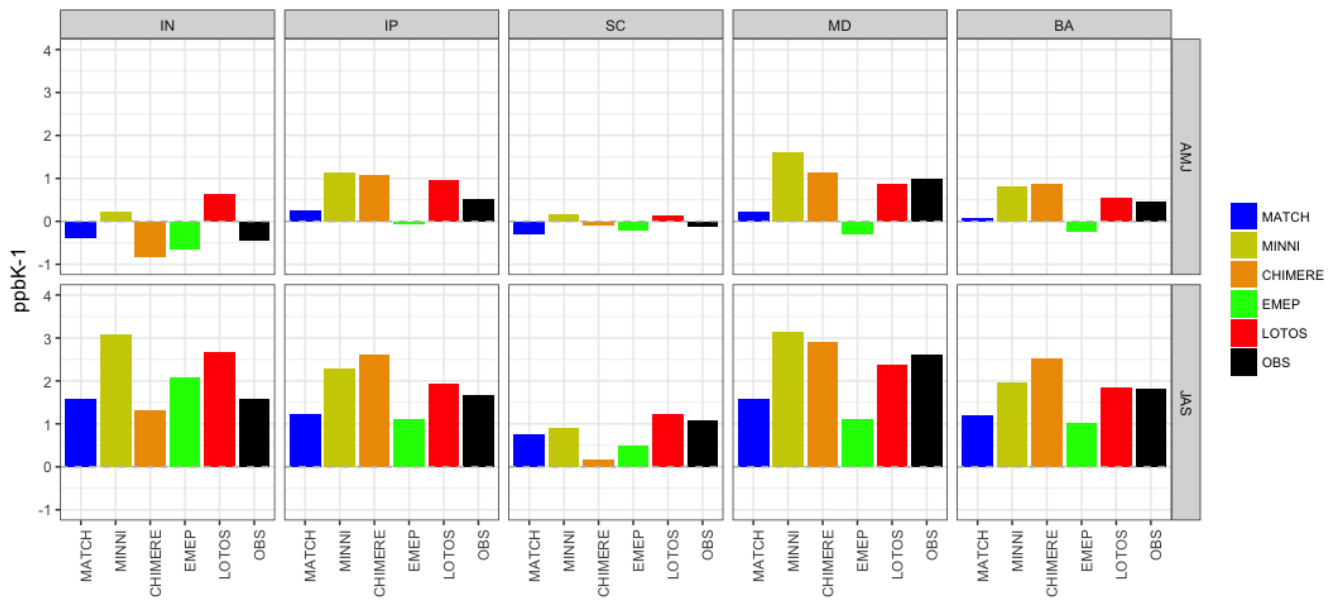
908
909
910
911
912
913
914

Figure 9. Standardised coefficients values of the main key-driving factors (LO3, Tx and RH) for each CTM-based (ordered as in Fig.3) and observation-based MLR in AMJ (top) and JAS (bottom) and for the external regions: Inflow (IN), Iberian Peninsula (IP), Scandinavia (SC), Mediterranean (ME) and Balkans (BA).



915
916
917
918
919
920

Figure 10. Slopes (m_{O_3-T} ; $ppbK^{-1}$) obtained from a simple linear regression to estimate the relationship ozone-temperature for each CTM-based (ordered as in Fig.3) and observation-based MLR in AMJ (top) and JAS (bottom) and for the internal regions: England (EN), France (FR), Mid-EU (ME), North Italy (NI), East-EU (EA).



921
 922
 923
 924
 925
 926
 927

Figure 11. Slopes (m_{O_3-T} ; $ppbK^{-1}$) obtained from a simple linear regression to estimate the relationship ozone-temperature for each CTM-based (ordered as in Fig.3) and observation-based MLR in AMJ (top) and JAS (bottom) and for the external regions: Inflow (IN), Iberian Peninsula (IP), Scandinavia (SC), Mediterranean (ME) and Balkans (BA).

928

929 **References**

930

931 Andersson, C., J. Langner, and R. Bergström: Interannual variation and trends in air
932 pollution over Europe due to climate variability during 1958–2001 simulated with a
933 regional CTM coupled to the ERA-40 reanalysis, *Tellus, Ser. B*, 59, 77–98, 2007.

934

935 Andersson C., Bergström R., Johansson C., Population exposure and mortality due to
936 regional background PM in Europe–Long-term simulations of source region and
937 shipping contributions, *Atmospheric Environment*, 43, 22, 3614-3620,
938 <http://dx.doi.org/10.1016/j.atmosenv.2009.03.040>, 2009.

939

940 Andersson, C. and Engardt, M.: European ozone in a future climate: Importance of
941 changes in dry deposition and isoprene emissions, *J. Geophys. Res.-Atmos.*, 115,
942 D02303, doi:10.1029/2008jd011690, 2010.

943

944 Baklanov, A., Schlünzen, K., Suppan, P., Baldasano, J., Brunner, D., Aksoyoglu, S.,
945 Carmichael, G., Douros, J., Flemming, J., Forkel, R., Galmarini, S., Gauss, M., Grell,
946 G., Hirtl, M., Joffre, S., Jorba, O., Kaas, E., Kaasik, M., Kallos, G., Kong, X.,
947 Korsholm, U., Kurganskiy, A., Kushta, J., Lohmann, U., Mahura, A., Manders-Groot,
948 A., Maurizi, A., Moussiopoulos, N., Rao, S. T., Savage, N., Seigneur, C., Sokhi, R. S.,
949 Solazzo, E., Solomos, S., Sørensen, B., Tsegas, G., Vignati, E., Vogel, B., and Zhang,
950 Y.: Online coupled regional meteorology chemistry models in Europe: current status
951 and prospects, *Atmos. Chem. Phys.*, 14, 317–398, doi:10.5194/acp-14-317-2014, 2014.

952

953 Barrero M A, Grimalt J O and Canton L.: Prediction of daily ozone concentration
954 maxima in the urban atmosphere *Chemometr. Intell. Lab. Syst.* 80 67–76, 2005.

955

956 Beltman, J. B., Hendriks, C., Tum, M., and Schaap, M.: The impact of large scale
957 biomass production on ozone air pollution in Europe, *Atmos. Environ.*, 71, 352–363,
958 2013.

959

960 Bessagnet, B., Pirovano, G., Mircea, M., Cuvelier, C., Aulinger, A., Calori, G., Ciarelli,
961 G., Manders, A., Stern, R., Tsyro, S., García Vivanco, M., Thunis, P., Pay, M.-T.,
962 Colette, A., Couvidat, F., Meleux, F., Rouïl, L., Ung, A., Aksoyoglu, S., Baldasano, J.
963 M., Bieser, J., Briganti, G., Cappelletti, A., D’Isidoro, M., Fi- nardi, S., Kranenburg, R.,
964 Silibello, C., Carnevale, C., Aas, W., Dupont, J.-C., Fagerli, H., Gonzalez, L., Menut,
965 L., Prévôt, A. S. H., Roberts, P., and White, L.: Presentation of the EURODELTA III
966 intercomparison exercise – evaluation of the chemistry transport models’ performance
967 on criteria pollutants and joint analysis with meteorology, *Atmos. Chem. Phys.*, 16,
968 12667–12701, doi:10.5194/acp-16-12667-2016, 2016.

969

970 Bloomfield P J, Royle J A, Steinberg L J and Yang Q: Accounting for meteorological
971 effects in measuring urban ozone levels and trends *Atmos. Environ.* 30 3067–77, 1996 .

972

973 Bloomer, B. J., Stehr, J. W., Piety, C. A., Salawitch, R. J., and Dickerson, R. R.:
974 Observed relationships of ozone air pollution with temperature and emissions, *Geophys.*
975 *Res. Lett.*, 36, L09803, doi:10.1029/2009gl037308, 2009.

976

977 Bott, A.: A Positive Definite Advection Scheme Obtained by Nonlinear
978 Renormalization of the Advective Fluxes, *Mon. Weather Rev.*, 117, 1006–1015, 1989.
979

980 Brown-Steiner, B., Hess, P. G., and Lin, M. Y.: On the capabilities and limitations of
981 GCM simulations of summertime regional air quality: A diagnostic analysis of ozone
982 and temperature simulations in the US using CESM CAM-Chem, *Atmos. Environ.*, 101,
983 134–148, doi:10.1016/j.atmosenv.2014.11.001, 2015.
984

985 Brunner, D., Jorba, O., Savage, N., Eder, B., Makar, P., Giordano, L., Badia, A.,
986 Balzarini, A., Baro, R., Bianconi, R., Chemel, C., Forkel, R., Jimenez-Guerrero, P.,
987 Hirtl, M., Hodzic, A., Honzak, L., Im, U., Knote, C., Kuenen, J. J. P., Makar, P. A.,
988 MandersGroot, A., Neal, L., Perez, J. L., Pirovano, G., San Jose, R., Savage, N.,
989 Schroder, W., Sokhi, R. S., Syrakov, D., Torian, A., Werhahn, K., Wolke, R., van
990 Meijgaard, E., Yahya, K., Zabkar, R., Zhang, Y., Zhang, J., Hogrefe, C., and Galmarini,
991 S.: Comparative analysis of meteorological performance of coupled chemistry-
992 meteorology models in the context of AQMEII phase 2, *Atmos. Environ.*, 115, 470–
993 498, 2015.
994

995 Camalier, L., Cox, W., and Dolwick, P.: The effects of meteorology on ozone in urban
996 areas and their use in assessing ozone trends, *Atmos. Environ.*, 41, 7127–7137, 2007.
997

998 Carro-Calvo, L., C. Ordóñez, R. García-Herrera, J. L. Schnell: Spatial clustering and
999 meteorological drivers of summer ozone in Europe, *Atmos. Environ.*, 167, 496-
1000 510, <https://doi.org/10.1016/j.atmosenv.2017.08.050>, 2017.
1001

1002 Chaloulakou A, Saisana M and Spyrellis N: Comparative assessment of neural networks
1003 and regression models for forecasting summertime ozone in Athens *Science of the Total*
1004 *Environment* 313 1–13, 2003.
1005

1006 Coates, J., Mar, K. A., Ojha, N., and Butler, T. M.: The influence of temperature on
1007 ozone production under varying NO_x conditions – a modelling study, *Atmos. Chem.*
1008 *Phys.*, 16, 11601-11615, <https://doi.org/10.5194/acp-16-11601-2016>, 2016.
1009

1010 Colette, A., Andersson, C., Baklanov, A., Bessagnet, B., Brandt, J., Christensen, J.,
1011 Doherty, R., Engardt, M., Geels, C., Giannakopoulos, C., Hedegaard, G., Katragkou, E.,
1012 Langner, J., Lei, H., Manders, A., Melas, D., Meleux, F., Rouil, L., Sofiev, M., Soares,
1013 J., Stevenson, D., Tombrou-Tzella, M., Varotsos, K., and Young, P.: Is the ozone
1014 climate penalty robust in Europe?, *Environ. Res. Lett.*, 10, 084015, doi:10.1088/1748-
1015 9326/10/8/084015, 2015.
1016

1017 Colette, A., Andersson, C., Manders, A., Mar, K., Mircea, M., Pay, M.-T., Raffort, V.,
1018 Tsyro, S., Cuvelier, C., Adani, M., Bessagnet, B., Bergström, R., Briganti, G., Butler,
1019 T., Cappelletti, A., Couvidat, F., D'Isidoro, M., Doumbia, T., Fagerli, H., Granier, C.,
1020 Heyes, C., Klimont, Z., Ojha, N., Otero, N., Schaap, M., Sindelarova, K., Stegehuis, A.
1021 I., Roustan, Y., Vautard, R., van Meijgaard, E., Vivanco, M. G., and Wind, P.:
1022 EURODELTA-Trends, a multi-model experiment of air quality hindcast in Europe over
1023 1990–2010, *Geosci. Model Dev. Discuss.*, <https://doi.org/10.5194/gmd-2016-309>,
1024 accepted, 2017a.
1025

1026 Colette, A., Solberg, S., Beauchamp, M., Bessagnet, B., Malherbe, L., and Guerreiro,

1027 C.: Long term air quality trends in Europe: Contribution of meteorological variability,
1028 natural factors and emissions, ETC/ACM, Bilthoven, 2017b.

1029

1030 Comrie A. C.: Comparing neural networks and regression models for ozone forecasting
1031 J. Air Waste Manage. Assoc. 47 653–63, 1997.

1032

1033 Dahlgren, P., Landelius, T., Kållberg, P., and Gollvik, S.: A high-resolution regional
1034 reanalysis for Europe. Part 1: Three-dimensional reanalysis with the regional HIgh-
1035 Resolution Limited-Area Model (HIRLAM), Quarterly Journal of the Royal
1036 Meteorological Society, 142, 2119-2131, 10.1002/qj.2807, 2016.

1037

1038 Davis, J., Cox, W., Reff, A., Dolwick, P.: A comparison of Cmaq-based and
1039 observation-based statistical models relating ozone to meteorological parameters.
1040 Atmospheric Environment 45, 3481e3487. [http://dx.doi.org/10.1016/](http://dx.doi.org/10.1016/J.Atmosenv.2010.12.060)
1041 [J.Atmosenv.2010.12.060](http://dx.doi.org/10.1016/J.Atmosenv.2010.12.060), 2011.

1042 Dawson, J.P., Adams, P.J., Pandis, S.N.: Sensitivity of ozone to summertime climate in
1043 the Eastern USA: a modeling case study. Atmos. Environ. 41, 1494– 1511, 2007.

1044

1045 Dawson, J. P., Racherla, P. N., Lynn, B. H., Adams, P. J., and Pan- dis, S. N.:
1046 Simulating present-day and future air quality as cli- mate changes: model evaluation,
1047 Atmos. Environ., 42, 4551– 4566, doi:10.1016/j.atmosenv.2008.01.058, 2008.

1048

1049 Dee D P et al. :The ERA-Interim reanalysis: configuration and performance of the data
1050 assimilation system Quart. J. R. Meteorol. Soc. 137 553–97, 2001.

1051

1052 Doherty, R. M., Wild, O., Shindell, D. T., Zeng, G., MacKenzie, I. A., Collins, W. J.,
1053 Fiore, A. M., Stevenson, D. S., Dentener, F. J., Schultz, M. G., Hess, P., Derwent, R.
1054 G., and Keating, T. J.: Impacts of climate change on surface ozone and intercontinental
1055 ozone pollution: a multi- model study, J. Geophys. Res.-Atmos., 118, 3744–3763,
1056 doi:10.1002/jgrd.50266, 2013.

1057

1058 Emberson, L. D., Ashmore, M. R., Simpson, D., Tuovinen, J.-P., and Cambridge, H.
1059 M.: Towards a model of ozone deposition and stomatal uptake over Europe, Norwegian
1060 Meteorological Institute, Oslo, Norway, 57, 2000a.

1061

1062 Emberson, L. D., Ashmore, M. R., Simpson, D., Tuovinen, J.-P., and Cambridge, H.
1063 M.: Modelling stomatal ozone flux across Europe, Water Air Soil Pollut., 109, 403–413,
1064 2000b.

1065

1066 Elminir H.K.: Dependence of urban air pollutants on meteorology, Science of The Total
1067 Environment, 350,225-237, <http://dx.doi.org/10.1016/j.scitotenv.2005.01.043>, 2005.

1068

1069 Fischer M., Rust H.W., and Ulbrich U.: Seasonality in extreme precipitation – using
1070 extreme value statistics to describe the annual cycle in german daily precipitation.
1071 Meteorol. Z. accepted, 2017.

1072

1073 Fiore, A. M., Dentener, F. J., Wild, O., Cuvelier, C., Schultz, M. G., Hess, P., Textor,
1074 C., Schulz, M., Doherty, R. M., Horowitz, L. W., MacKenzie, I. A., Sanderson, M. G.,
1075 Shindell, D. T., Stevenson, D. S., Szopa, S., Van Dingenen, R., Zeng, G., Atherton, C.,

1076 Bergmann, D., Bey, I., Carmichael, G., Collins, W. J., Duncan, B. N., Faluvegi, G.,
1077 Folberth, G., Gauss, M., Gong, S., Hauglustaine, D., Holloway, T., Isaksen, I. S. A.,
1078 Jacob, D. J., Jonson, J. E., Kaminski, J. W., Keating, T. J., Lupu, A., Marmer, E.,
1079 Montanaro, V., Park, R. J., Pitari, G., Pringle, K. J., Pyle, J. A., Schroeder, S., Vivanco,
1080 M. G., Wind, P., Wojcik, G., Wu, S., and Zuber, A.: Multimodel estimates of
1081 intercontinental source-receptor relationships for ozone pollution, *J. Geophys. Res.-*
1082 *Atmos.*, 114, D04301, doi:10.1029/2008jd010816, 2009.

1083

1084 Fix, M. J., D. Cooley, A. Hodzic, E. Gilleland, B. T. Russell, W. C. Porter, and G. G.
1085 Pfister, 2018: Observed and predicted sensitivities of extreme surface ozone to
1086 meteorological drivers in three US cities. *Atmospheric Environment*, 176, 292-300,
1087 doi:10.1016/j.atmosenv.2017.12.036.

1088 Gan C., Hogrefe C., Mathur R., Pleim J., Xing J., Wong D., Gilliam R., Pouliot G., Wei
1089 C.: Assessment of the effects of horizontal grid resolution on long-term air quality
1090 trends using coupled WRF-CMAQ simulations, *Atmospheric Environment*, 132, 207-
1091 216,1352-2310,https://doi.org/10.1016/j.atmosenv.2016.02.036., 2016.

1092

1093 Grell, G. A., Peckham, S. E., Schmitz, R., McKeen, S. A., Frost, G., Skamarock, W. C.,
1094 and Eder, B.: Fully coupled “online” chemistry within the WRF model, *Atmospheric*
1095 *Environment*, 39, 6957-6975, http://dx.doi.org/10.1016/j.atmosenv.2005.04.027, 2005.

1096

1097 Grömping U.: Estimators of relative importance in linear regression based on variance
1098 decomposition *Am. Stat.* 61 139–47, 2007.

1099

1100 Guenther, A., Zimmerman, P., Harley, P., Monson, R., and Fall, R.: Isoprene and
1101 monoterpene rate variability: model evaluations and sensitivity analyses, *J. Geophys.*
1102 *Res.*, 98, 12609–12617, 1993.

1103

1104 Guenther, A., Zimmerman, P., and Wildermuth, M.: Natural volatile organic compound
1105 emission rate estimates for US woodland landscapes, *Atmos. Environ.*, 28, 1197–1210,
1106 1994.

1107

1108 Guenther, A., Karl, T., Harley, P., Wiedinmyer, C., Palmer, P. I., and Geron, C.:
1109 Estimates of global terrestrial isoprene emissions using MEGAN (Model of Emissions
1110 of Gases and Aerosols from Nature), *Atmos. Chem. Phys.*, 6, 3181–3210,
1111 doi10.5194/acp-6-3181-2006, 2006.

1112

1113 Hedegaard, G. B., Christensen, J. H., and Brandt, J.: The relative importance of impacts
1114 from climate change vs. emissions change on air pollution levels in the 21st century,
1115 *Atmos. Chem. Phys.*, 13, 3569-3585, doi:10.5194/acp-13-3569-2013, 2013.

1116

1117 Hendriks C., Forsell N., Kiesewetter G., Schaap M., Schöpp W.: Ozone concentrations
1118 and damage for realistic future European climate and air quality scenarios, *Atmospheric*
1119 *Environment*, 144, 208-219, http://dx.doi.org/10.1016/j.atmosenv.2016.08.026, 2016.

1120

1121 Hodnebrog, Ø., Solberg, S., Stordal, F., Svendby, T. M., Simpson, D., Gauss, M.,
1122 Hilboll, A., Pfister, G. G., Turquety, S., Richter, A., Burrows, J. P., and Denier van der
Gon, H. A. C.: Impact of forest fires, biogenic emissions and high temperatures on the

1123 elevated Eastern Mediterranean ozone levels during the hot summer of 2007, *Atmos.*
1124 *Chem. Phys.*, 12, 8727-8750, <https://doi.org/10.5194/acp-12-8727-2012>, 2012
1125
1126 Hogrefe, C., Biswas, J., Lynn, B., Civerolo, K., Ku, J. Y., Rosenthal, J., Rosenzweig,
1127 C., Goldberg, R., and Kinney, P. L.: Simulating regional-scale ozone climatology over
1128 the eastern United States: model evaluation results, *Atmos. Environ.*, 38, 2627–2638,
1129 2004.
1130
1131 IPCC, Climate Change 2013, the Physical Science Basis. Working Group I contribution
1132 to the fifth assessment report of the Intergovernmental Panel on Climate
1133 Change, Cambridge University Press, 2013.
1134
1135 Jacob, D. J. and Winner, D. A.: Effect of climate change on air quality, *Atmos.*
1136 *Environ.*, 43, 51–63, doi:10.1016/j.atmosenv.2008.09.051, 2009.
1137
1138 Jericevic, A., Kraljevic, L., Grisogono, B., Fagerli, H., and Vecenaj, Ž.:
1139 Parameterization of vertical diffusion and the atmospheric boundary layer height
1140 determination in the EMEP model, *Atmos. Chem. Phys.*, 10, 341–364,
1141 <https://doi.org/10.5194/acp-10-341-2010>, 2010.
1142
1143 Jonson, J. E., Simpson, D., Fagerli, H., and Solberg, S.: Can we explain the trends in
1144 European ozone levels?, *Atmos. Chem. Phys.*, 6, 51–66, doi:10.5194/acp-6-51-2006,
1145 2006.
1146
1147 Kavassalis, S. C., and J. G. Murphy: Understanding ozone-meteorology correlations: A
1148 role for dry deposition, *Geophys. Res. Lett.*, 44, 2922–2931,
1149 doi:10.1002/2016GL071791, 2017.
1150
1151 Koeble, R. and Seufert, G.: Novel Maps for Forest Tree Species in Europe, A Changing
1152 Atmosphere, 8th European Symposium on the Physico-Chemical Behaviour of
1153 Atmospheric Pollutants, Torino, Italy, 2001.
1154
1155 Kong, X., Forkel R., Sokhi R. S., Suppan P., Baklanov A., Gauss M., Brunner D., Barò
1156 R., Balzarini A., Chemel C., Curci G., Jiménez-Guerrero P., Hirtl M., Honzak L., Im U.,
1157 Pérez J. L., Pirovano G., San Jose R., Schlünzen K. H. , Tsegas G., Tuccella P.,
1158 Werhahn J., Žabkar R., Galmarini S.: Analysis of Meteorology-Chemistry Interactions
1159 During Air Pollution Episodes Using Online Coupled Models within AQMEII Phase-2,
1160 *Atmospheric Environment*, <http://dx.doi.org/10.1016/j.atmosenv.2014.09.020>., 2014.
1161
1162 Kutner M. H., Nachtsheim C. J. and Neter J.: *Applied Linear Regression Models* 4th Ed
1163 (Boston, MA: McGraw-Hill Irwin) 2004.
1164
1165 Lange, R.: Transferrability of a three-dimensional air quality model between two
1166 different sites in complex terrain, *J. Appl. Meteorol.*, 78, 665–679, 1989.
1167
1168 Langner, J., Bergström R. and Foltescu V.: Impact of climate change on surface ozone
1169 and deposition of sulphur and nitrogen in Europe, *Atmos. Environ.*, 39, 1129–1141,
1170 doi:10.1016/j.atmosenv.2004.09.082, 2005.
1171
1172 Lelieveld, J., and P. J. Crutzen: Influence of cloud and photochemical processes on

1172 tropospheric ozone, *Nature*, 343, 227–233, 1990.

1173 Lemaire, V. E. P., Colette, A. and Menut, L.: Using statistical models to explore
 1174 ensemble uncertainty in climate impact studies: the example of air pollution in Europe,
 1175 *Atmos. Chem. Phys.*, 16, 2559–2574, doi:10.5194/acp-16-2559-2016, 2016.

1176

1177 Lindeman R.H. , Merenda P. F. and Gold RZ: *Introduction to Bivariate and Multivariate*
 1178 *Analysis*. Scott, Foresman, Glenview, IL, 1980.

1179

1180 Linderson M. L.: Objective classification of atmospheric circulation over southern
 1181 Scandinavia *Int. J. Climatol.* 21 155–69, 2001.

1182

1183 Mailler, S., Menut, L., Khvorostyanov, D., Valari, M., Couvidat, F., Siour, G.,
 1184 Turquety, S., Briant, R., Tuccella, P., Bessagnet, B., Colette, A., Létinois, L., Markakis,
 1185 K., and Meleux, F.: CHIMERE-2017: from urban to hemispheric chemistry-transport
 1186 modeling, *Geosci. Model Dev.*, 10, 2397–2423, [https://doi.org/10.5194/gmd-10-2397-](https://doi.org/10.5194/gmd-10-2397-2017)
 1187 2017, 2017.

1188 Maindonald J, Braun J: *Data analysis and graphics using R: an example-based*
 1189 *approach*.Cambridge (United Kingdom), Cambridge University Press, 2006.

1190

1191 Makar, P.A., Gong,W., Hogrefe, C., Zhang, Y., Curci, G., Zakbar, R., Milbrandt, J., Im,
 1192 U., Galmarini, S., Gravel, S., Zhang, J., Hou, A., Pabla, B., Cheung, P., Bianconi, R.,
 1193 2015b. Feedbacks between Air Pollution and Weather, Part 1: Effects on Weather.
 1194 *Atmos. Environ.* 115, 442e469.

1195

1196 Manders, A. M. M., van Meijgaard, E., Mues, A. C., Kranenburg, R., van Ulft, L. H.,
 1197 and Schaap, M.: The impact of differences in large-scale circulation output from climate
 1198 models on the regional modeling of ozone and PM, *Atmos. Chem. Phys.*, 12, 9441–
 1199 9458, doi:10.5194/acp-12-9441-2012, 2012.

1200

1201 Manders, A. M. M., Builtjes, P. J. H., Curier, L., Denier van der Gon, H. A.
 1202 C., Hendriks, C., Jonkers, S., Kranenburg, R., Kuenen, J., Segers, A. J.,
 1203 Timmermans, R. M. A., Visschedijk, A., Wichink Kruit, R. J., Van Pul, W. A. J.,
 1204 Sauter, F. J., van der Swaluw, E., Swart, D. P. J., Douros, J., Eskes, H., van
 1205 Meijgaard, E., van Ulft, B., van Velthoven, P., Banzhaf, S., Mues, A., Stern, R.,
 1206 Fu, G., Lu, S., Heemink, A., van Velzen, N., and Schaap, M.: Curriculum Vitae of
 1207 the LOTOS-EUROS (v2.0) chemistry transport model, *Geosci. Model Dev. Discuss.*,
 1208 <https://doi.org/10.5194/gmd-2017-88>, in review, 2017.

1209

1210 Meijgaard, E. v., van Ulft, L. H., Lenderink, G., de Roode, S. R., Wipfler, L., Boers, R.,
 1211 and Timmermans, R. M. A.: Refinement and application of a regional atmospheric
 1212 model for climate scenario calculations of Western Europe, *KvR 054/12*, 44, 2012.

1213

1214 Meleux, F., Solmon, F., and Giorgi, F.: Increase in summer European ozone amounts
 1215 due to climate change, *Atmos. Environ.*, 41, 7577–7587,
 1216 doi:10.1016/j.atmosenv.2007.05.048, 2007.

1217

1218 Millán, M. M., Sanz, M. J., Salvador, R., and Mantilla, E.: Atmospheric dynamics and
 1219 ozone cycles related to nitrogen deposition in the western Mediterranean, *Environ.*

1220 Pollut., 118, 167–186, 2002.
1221
1222 Mills, G., Hayes, F., Jones, M. L. M., and Cinderby, S.: Identifying ozone-sensitive
1223 communities of (semi-)natural vegetation suitable for mapping exceedance of critical
1224 levels, *Environ. Pollut.*, 146, 736–743, doi:10.1016/j.envpol.2006.04.005, 2007.
1225
1226 Mircea, M., Grigoras, G., D’Isidoro, M., Righini, G., Adani, M., Briganti, G.,
1227 Ciancarella, L., Cappelletti, A., Calori, G., Cionni, I., Cremona, G., Finardi, S., Larsen,
1228 B. R., Pace, G., Perrino, C., Piersanti, A., Silibello, C., Vitali, L., and Zanini, G.: Impact
1229 of grid resolution on aerosol predictions: a case study over Italy, *Aerosol and Air*
1230 *Quality Research*, 1253–1267, doi: 10.4209/aaqr.2015.02.0058, 2016.
1231
1232 Monks, P. S.: A review of the observations and origins of the spring ozone maximum,
1233 *Atmos. Environ.*, 34, 3545–3561, 2000.
1234
1235 Monks, P. S., Archibald, A. T., Colette, A., Cooper, O., Coyle, M., Derwent, R.,
1236 Fowler, D., Granier, C., Law, K. S., Mills, G. E., Stevenson, D. S., Tarasova, O.,
1237 Thouret, V., von Schneidmesser, E., Sommariva, R., Wild, O., and Williams, M. L.:
1238 Tropospheric ozone and its precursors from the urban to the global scale from air
1239 quality to short-lived climate forcer, *Atmos. Chem. Phys.*, 15, 8889-8973,
1240 <https://doi.org/10.5194/acp-15-8889-2015>, 2015.
1241
1242 O’Brien, J. J.: A note on the vertical structure of the eddy Exchange coefficient in the
1243 planetary boundary layer, *J. Atmos. Sci.*, 27, 1213–1215, 1970.
1244
1245 Ordóñez, C., Mathis, H., Furger, M., Henne, S., Hoglin, C., Staehelin, J., Prevot,
1246 A.S.H.: Changes of daily surface ozone maxima in Switzerland in all seasons from 1992
1247 to 2002 and discussion of summer 2003. *Atmos. Chem. Phys.* 5, 1187– 1203, 2005.
1248
1249 Ordóñez, C., Barriopedro, D., García-Herrera, R., Sousa, P. M., and Schnell, J. L.:
1250 Regional responses of surface ozone in Europe to the location of high-latitude blocks
1251 and subtropical ridges, *Atmos. Chem. Phys.*, 17, 3111-3131,
1252 <https://doi.org/10.5194/acp-17-3111-2017>, 2017.
1253
1254 Otero, N., Sillmann, J., Schnell, J.L., Rust, H.W., Butler, T., 2016. Synoptic and
1255 meteorological drivers of extreme ozone concentrations over Europe. *Environ. Res.*
1256 *Lett.* 11 (2), 24005. <http://dx.doi.org/10.1088/1748-9326/11/2/024005>.
1257
1258 Porter W C, Heald C L, Cooley D and Russell B 2015 Investigating the observed
1259 sensitivities of air quality extremes to meteorological drivers via quantile regression
1260 *Atmos. Chem. Phys. Discuss.* 15 10349–66, 2015.
1261
1262 Pusede S E et al. : On the temperature dependence of organic reactivity, nitrogen
1263 oxides, ozone production, and the impact of emission controls in San Joaquin Valley,
1264 California *Atmos. Chem. Phys.* 14 3373–95, 2014.
1265
1266 Querol, X., Gangoiti, G., Mantilla, E., Alastuey, A., Minguillón, M. C., Amato, F.,
1267 Reche, C., Viana, M., Moreno, T., Karanasiou, A., Rivas, I., Pérez, N., Ripoll, A.,
1268 Brines, M., Ealo, M., Pandolfi, M., Lee, H.-K., Eun, H.-R., Park, Y.-H., Escudero, M.,
1269 Beddows, D., Harrison, R. M., Bertrand, A., Marchand, N., Lyasota, A., Codina, B.,

1270 Olid, M., Udina, M., Jiménez-Esteve, B., Soler, M. R., Alonso, L., Millán, M., and Ahn,
1271 K.-H.: Phenomenology of high-ozone episodes in NE Spain, *Atmos. Chem. Phys.*, 17,
1272 2817-2838, <https://doi.org/10.5194/acp-17-2817-2017>, 2017.
1273

1274 Rasmussen, D. J., Fiore, A. M., Naik, V., Horowitz, L. W., McGinnis, S. J., and
1275 Schultz, M. G.: Surface ozone-temperature relationships in the eastern US: A monthly
1276 climatology for evaluating chemistry-climate models, *Atmos. Environ.*, 47, 142–153,
1277 doi:10.1016/j.atmosenv.2011.11.021, 2012.
1278

1279 Robertson, L., Langner, J., and Engardt, M.: An Eulerian Limited-Area Atmospheric
1280 Transport Model, *Journal of Applied Meteorology*, 38, 190-210, 1999.
1281

1282 Rust H, Maraun D. and Osborn T.: Modelling seasonality in extreme precipitation *Eur.*
1283 *Phys. J. Special Topics* 174 99–111, 2009.
1284

1285 Rust H. W., Vrac M., Sultan B., and Lengaigne M.: Mapping weather-type influence on
1286 Senegal precipitation based on a spatial-temporal statistical model. *J. Climate*, 26:8189–
1287 8209. ISSN 0894-8755. URL <http://dx.doi.org/10.1175/JCLI-D-12-00302.1.1>. 2013
1288

1289 Schaap, M., Timmermans, R. M. A., Roemer, M., Boersen, G. A. C., Builtjes, P.,
1290 Sauter, F., Velders, G., and Beck, J.: The LOTOS-EUROS model: description,
1291 validation and latest developments, *International Journal of Environment and Pollution*,
1292 32, 270-290, 2008.
1293

1294 Schaap M., Cuvelier C, Hendriks C., Bessagnet B., Baldasano J.M., Colette A., Thunis
1295 P., Karam D., Fagerli H., Graff A., Kranenburg R., Nyiri A., Pay M.T., Rouil L., Schulz
1296 M., Simpson D., Stern R., Terrenoire E., Wind P.: Performance of European chemistry
1297 transport models as function of horizontal resolution, *Atmospheric Environment*, 112,
1298 90-105, <http://dx.doi.org/10.1016/j.atmosenv.2015.04.003>, 2015.
1299

1300 Skamarock, W. C., Klemp, J. B., Dudhia, J., Gill, D. O., Barker, D. M., Duda, M. G.,
1301 Huang, X. Y., Wang, W., and Powers, J. G.: A Description of the Advanced Research
1302 WRF Version 3, NCAR, 2008.
1303

1304 Schnell, J. L., Holmes, C. D., Jangam, A., and Prather, M. J.: Skill in forecasting
1305 extreme ozone pollution episodes with a global atmospheric chemistry model, *Atmos.*
1306 *Chem. Phys.*, 14, 7721–7739, doi:10.5194/acp-14-7721-2014, 2014.
1307

1308 Schnell, J. L., Prather, M. J., Josse, B., Naik, V., Horowitz, L. W., Cameron-Smith, P.,
1309 Bergmann, D., Zeng, G., Plummer, D. A., Sudo, K., Nagashima, T., Shindell, D. T.,
1310 Faluvegi, G., and Strode, S. A.: Use of North American and European air quality
1311 networks to evaluate global chemistry–climate modeling of surface ozone, *Atmos.*
1312 *Chem. Phys.*, 15, 10581-10596, doi:10.5194/acp-15-10581-2015, 2015.
1313

1314 Seo, J., Youn, D., Kim, J. Y., and Lee, H.: Extensive spatiotemporal analyses of surface
1315 ozone and related meteorological variables in South Korea for the period 1999–2010,
1316 *Atmos. Chem. Phys.*, 14, 6395-6415, <https://doi.org/10.5194/acp-14-6395-2014>, 2014.
1317

1318 Sillman, S. and Samson, P.J: Impact of temperature on oxidant photochemistry in
1319 urban, polluted rural and remote environments. *Journal of Geophysical Research* 100:

1320 doi: 10.1029/94JD02146. issn: 0148-0227, 1995.
1321
1322 Simpson, D., Guenther, A., Hewitt, C., and Steinbrecher, R.: Biogenic emissions in
1323 Europe 1. Estimates and uncertainties, *J. Geophys. Res.*, 100, 22875–22890, 1995.
1324
1325 Simpson, D., Benedictow, A., Berge, H., Bergström, R., Emberson, L. D., Fagerli, H.,
1326 Flechard, C. R., Hayman, G. D., Gauss, M., Jonson, J. E., Jenkin, M. E., Nyíri, A.,
1327 Richter, C., Semeena, V. S., Tsyro, S., Tuovinen, J.-P., Valdebenito, Á., and Wind, P.:
1328 The EMEP MSC-W chemical transport model – technical description, *Atmos. Chem.*
1329 *Phys.*, 12, 7825–7865, <https://doi.org/10.5194/acp-12-7825-2012>, 2012
1330
1331 Simpson, D., Andersson, C., Christensen, J. H., Engardt, M., Geels, C., Nyiri, A.,
1332 Posch, M., Soares, J., Sofiev, M., Wind, P., and Langner, J.: Impacts of climate and
1333 emission changes on nitrogen deposition in Europe: a multi-model study, *Atmos. Chem.*
1334 *Phys.*, 14, 6995-7017, <https://doi.org/10.5194/acp-14-6995-2014>, 2014.
1335
1336 Smyth, S., Yin, D., Roth, H., Jiang, W., Moran, M.D., Crevier, L.P., 2006. The impact
1337 of GEM and MM5 meteorology on CMAQ air quality modeling results in eastern
1338 Canada and the northeastern United States. *Journal of Applied Meteorology* 45,
1339 1525e1541. doi:10.1175/JAM2420.1.
1340
1341 Solberg, S., R. G. Derwent, Ø. Hov, J. Langner, and A. Lindskog: European abatement
1342 of surface ozone in a global perspective, *Ambio*, 34, 47–53, 2005.
1343
1344 Solberg, S., Hov, Ø., Sovde, A., Isaksen, I. S. A., Coddeville, P., De Backer, H.,
1345 Forster, C., Orsolini, Y., and Uhse, K.: European surface ozone in the extreme summer
1346 2003, *J. Geophys. Res. Atmos.*, 113, D07307, doi:10.1029/2007jd009098, 2008.
1347
1348 Solberg, S., Colette, A., and Guerreiro, C. B. B.: Discounting the impact of meteorology
1349 to the ozone concentration trends. ETC/ACM, NILU, INERIS.
1350 <https://doi.org/10.13140/rg.2.2.15389.92649>, 2016.
1351
1352 Steiner, A.L., Tonse, S., Cohen, R.C., Goldstein, A.H., Harley, R.A.: Influence of
1353 future climate and emissions on Regional air quality in California. *Journal of*
1354 *Geophysical Research-Atmospheres* 111, 2006.
1355
1356 Vautard, R., Honore, C., Beekmann, M., and Rouil, L.: Simulation of ozone
1357 during the August 2003 heat wave and emission control scenarios, *Atmos.*
1358 *Environ.*, 39, 2957–2967, doi:10.1016/j.atmosenv.2005.01.039, 2005.
1359
1360 Tang L., Chen D.L., Karlsson P.E., Gu Y.F., Ou T.H. Synoptic circulation and its
1361 influence on spring and summer surface ozone concentrations in Southern Sweden
1362 *Boreal Environment Research*, 14, 889-902, 2009.
1363
1364 Tarasova, O. A., Brenninkmeijer, C. A. M., Jöckel, P., Zvyagintsev, A. M., and
1365 Kuznetsov, G. I.: A climatology of surface ozone in the extra tropics: cluster analysis of
1366 observations and model results, *Atmos. Chem. Phys.*, 7, 6099–6117, doi:10.5194/acp-7-
1367 6099-2007, 2007.
1368
1369 Thompson M L, Reynolds J, Cox L H, Guttorp P and Sampson P D: A review of

1370 statistical methods for the meteorological adjustment of tropospheric ozone *Atmos.*
1371 *Environ.* 35 617–30, 2001.

1372

1373 Troen, I. and Mahrt, L.: A simple model of the atmospheric boundary layer: Sensitivity
1374 to surface evaporation, *Bound.-Lay. Meteorol.*, 37, 129–148, 1986.

1375

1376 Tuovinen, J.-P., Ashmore, M., Emberson, L., and Simpson, D.: Testing and improving
1377 the EMEP ozone deposition module, *Atmos. Environ.*, 38, 2373–2385, 2004.

1378

1379 van Loon, M., Vautard, R., Schaap, M., Bergström, R., Bessagnet, B., Brandt, J.,
1380 Bultjes, P. J. H., Christensen, J. H., Cuvelier, C., Graff, A., Jonson, J. E., Krol, M.,
1381 Langner, J., Roberts, P., Rouil, L., Stern, R., Tarrasón, L., Thunis, P., Vignati, E.,
1382 White, L., and Wind, P.: Evaluation of long-term ozone simulations from seven regional
1383 air quality models and their ensemble, *Atmospheric Environment*, 41, 2083–2097, 2007.

1384

1385 Vautard, R., Moran, M.D., Solazzo, E., Gilliam, R.C., Matthias, V., Bianconi, R.,
1386 Chemel, C., Ferreira, J., Geyer, B., Hansen, A.B., Jericevic, A., Prank, M., Segers, A.,
1387 Silver, J.D., Werhahn, J., Wolke, R., Rao, S.T., Galmarini, S., 2012. Evaluation of the
1388 meteorological forcing used for the Air Quality Model Evaluation International
1389 Initiative (AQMEII) air quality simulations. *Atmos. Environ.* 53, 15e37.

1390

1391 van Leer, B.: Multidimensional explicit difference schemes for hyperbolic conservation
1392 laws, in: *Computing Methods in Applied Sciences and Engineering VI*, edited by:
1393 Lions, R. G. A. J. L., Elsevier, Amsterdam, 1984.

1394

1395 Van Zanten, M. C., Sauter, F. J., Wichink Kruit, R. J., Van Jaarsveld, J. A., and Van Pul,
1396 W. A. J.: Description of the DEPAC module: 75 Dry deposition modelling with
1397 DEPAC_GC2010, Bilthoven, the Netherlands, 2010.

1398

1399 Walcek, C. J.: Minor flux adjustment near mixing ratio extremes for simplified yet
1400 highly accurate monotonic calculation of tracer advection, *J. Geophys. Res.*, 105, 9335–
1401 9348, 2000.

1402

1403 Wesely, M. L.: Parameterization of surface resistances to gaseous dry deposition in
1404 regional-scale numerical models, *Atmos. Environ.*, 23, 1293–1304, 1989.

1405

1406 Wilson, R. C., Fleming, Z. L., Monks, P. S., Clain, G., Henne, S., Konovalov, I. B.,
1407 Szopa, S., and Menut, L.: Have primary emission reduction measures reduced ozone
1408 across Europe? An analysis of European rural background ozone trends 1996–2005,
1409 *Atmos. Chem. Phys.*, 12, 437–54, <https://doi.org/10.5194/acp-12-437-2012>, 2012.

1410

1411 Wu, S., Mickley, L. J., Leibensperger, E. M., Jacob, D. J., Rind, D., and Streets, D. G.:
1412 Effects of 2000–2050 global change on ozone air quality in the United States, *J.*
1413 *Geophys. Res.-Atmos.*, 113, D18312, doi:10.1029/2007JD009639, 2008.

1414

1415 Yamartino, R. J., J. Flemming, and R.M. Stern: Adaptation of analytic diffusivity
1416 formulations to Eulerian grid model layers of finite thickness. In *27th ITM on Air*
1417 *Pollution Modelling and its Application*. Banff, Canada. 2004.

1418

1419 Yuan, H., Dai, Y., Xiao, Z., Ji, D., and Shangguan, W.: Reprocessing the MODIS Leaf

1420 Area Index Products for Land Surface and Climate Modelling, *Remote Sens. Environ.*,
1421 155, 1171–1187, <https://doi.org/10.1016/j.rse.2011.01.001>, 2011.
1422
1423 Zhang, L., Gong, S., Padro, J., and Barrie, L.: A size-segregated particle dry deposition
1424 scheme for an atmospheric aerosol module, *Atmos. Environ.*, 35, 549–560, 2001.
1425
1426 Zhang, Y.: Online-coupled meteorology and chemistry models: his- tory, current status,
1427 and outlook, *Atmos. Chem. Phys.*, 8, 2895– 2932, doi:10.5194/acp-8-2895-2008, 2008.
1428